

# Lévy flights in quenched random force fields

Hans C. Fogedby

*\* Institute of Physics and Astronomy, University of Aarhus, DK-8000, Aarhus C, Denmark  
and*

*NORDITA, Blegdamsvej 17, DK-2100, Copenhagen Ø, Denmark  
(February 5, 2018)*

Lévy flights, characterized by the microscopic step index  $f$ , are for  $f < 2$  (the case of rare events) considered in short range and long range quenched random force fields with arbitrary vector character to first loop order in an expansion about the critical dimension  $2f - 2$  in the short range case and the critical fall-off exponent  $2f - 2$  in the long range case. By means of a dynamic renormalization group analysis based on the momentum shell integration method, we determine flows, fixed point, and the associated scaling properties for the probability distribution and the frequency and wave number dependent diffusion coefficient. Unlike the case of ordinary Brownian motion in a quenched force field characterized by a single critical dimension or fall-off exponent  $d = 2$ , two critical dimensions appear in the Lévy case. A critical dimension (or fall-off exponent)  $d = f$  below which the diffusion coefficient exhibits anomalous scaling behavior, i.e. algebraic spatial behavior and long time tails, and a critical dimension (or fall-off exponent)  $d = 2f - 2$  below which the force correlations characterized by a non trivial fixed point become relevant. As a general result we find in all cases that the dynamic exponent  $z$ , characterizing the mean square displacement, locks onto the Lévy index  $f$ , *independent* of dimension and *independent* of the presence of weak quenched disorder.

PACS numbers: 05.40.+j, 64.60.Ht, 05.70.Ln, 68.35.Fx

## I. INTRODUCTION

There is a current interest in the dynamics of fluctuating manifolds in quenched random environments [1]. This fundamental issue in modern condensed matter physics is encountered in problems as diverse as vortex motion in high temperature superconductors, moving interfaces in porous media, and random field magnets and spin glasses. In this context the simplest case is that of a random walker in a random environment, corresponding to a zero dimensional fluctuating manifold. This problem has been treated extensively in the literature [2–4] and many results are known.

In the case of ordinary Brownian motion, characterized by a finite mean square step, in a pure environment without disorder, the central limit theorem [5] implies that the statistics of the walk is given by a Gaussian distribution with a mean square deviation proportional to the number of steps or, equivalently, the elapsed time, i.e., the mean square displacement is

$$\langle r^2(t) \rangle \propto Dt^{2/z}, \quad (1.1)$$

where the dynamic exponent  $z$  assumes the value  $z = 2$  for Brownian walk;  $D$  is the effective diffusion coefficient for the process and  $\langle \cdots \rangle$  denotes an ensemble average.

There are, however, many interesting processes in nature which are characterized by *anomalous diffusion* with dynamic exponent  $z \neq 2$ , owing to the statistical properties of the environments [3,4]. Examples are found in chaotic systems [6], turbulence [7,8], flow in fractal geometries [9], and Lévy flights [10,11]; these cases generally lead to enhanced diffusion or superdiffusion with  $z < 2$ ; we note that the ballistic case corresponds to  $z = 1$ . The other case of subdiffusion or dispersive behavior with  $z > 2$  is encountered in various constrained systems such as doped crystals, glasses or fractals [12–16].

Independent of the spatial dimension  $d$ , ordinary Brownian motion traces out a manifold of fractal dimension  $d_F = 2$  [17]. In the presence of a quenched disordered force field in  $d$  dimensions the Brownian walk is unaffected for  $d > d_F$ , i.e., for  $d$  larger than the critical dimension  $d_{c1} = d_F$  the walk is transparent and the dynamic exponent  $z$  locks onto the value 2 for the pure case. Below the critical dimension  $d_{c1} = 2$  the long time characteristics of the walk is changed to subdiffusive behavior with  $z > 2$  [18–20]. In  $d = 1$ ,  $\langle r^2(t) \rangle \propto [\log t]^4$ , independent of the strength of the quenched disorder [21].

---

\*Permanent address

Lévy flights constitute an interesting generalization of ordinary Brownian walks. Here the step size is drawn from a Lévy distribution characterized by the step index  $f$  [5,11]. The Lévy distribution has a long range algebraic tail corresponding to large but infrequent steps, so-called *rare events*. This step distribution has the interesting property that the central limit theorem does not hold in its usual form. For  $f > 2$  the second moment or mean square deviation of the step distribution is finite, the central limit theorem holds, and the dynamic exponent  $z$  for the Lévy walk locks onto 2, corresponding to ordinary diffusive behavior; however, for  $f < 2$  the mean square step deviation diverges, the rare large step events prevail determining the long time behavior, and the dynamic exponent  $z$  depends on the microscopic step index  $f$  according to the relationship  $z = f$  ( $f < 2$ ), indicating anomalous enhanced diffusion, that is superdiffusion [11,22,23]. The “built in” superdiffusive character of Lévy flights has been used to model a variety of physical processes such as self diffusion in micelle systems [24] and transport in heterogeneous rocks [22].

In a recent letter [25] we considered Lévy flights in the presence of a quenched isotropic random force field and examined the interplay between the “built in” superdiffusive behavior of the Lévy flights and the pinning effect of the random environment generally leading to subdiffusive behavior. Generalizing the discussion in [18,20,26] we found that in the case of enhanced diffusion for  $f < 2$  the dynamic exponent  $z$  locks onto  $f$ , *independent* of the presence of weak disorder. On the other hand, we could still identify a critical dimension  $d_{c1} = 2f - 2$ , depending on the step index  $f$  for  $f < 2$ . Below  $d_{c1}$  the quenched disorder becomes *relevant* as indicated by the emergence of a non-trivial fixed point in the renormalization group analysis. We also briefly discussed the behavior of the subleading diffusive term. Here another critical dimension,  $d_{c2} = f$  enters in the sense that for dimensions less than  $d_{c2}$  the correction to the ordinary diffusion coefficient diverges. This feature has also been discussed from a heuristic point of view in ref. [27]. Note that in the Brownian case for  $f = 2$  the critical dimensions coincide, i.e.,  $d_{c1} = d_{c2}$ .

In the present paper we discuss in more detail Lévy flights in quenched random force field with arbitrary range and vector character thus corroborating and extending the results obtained in ref. [25]. The paper is organized in the following manner. In Sec. II we introduce and discuss Lévy flights in a pure environment. Next we derive the Langevin equation for Lévy flights in a force field and the associated Fokker Planck equation for the probability distribution. In Sec. III we establish perturbation theory for the probability distribution in the Fokker Planck equation averaged over the quenched random force field and set up the renormalization group analysis. In order to extract the scaling properties and control divergent contributions we dilute the degrees of freedom by means of the momentum shell integration method. Finally we derive differential renormalization group equations to first loop order for the parameters in the model. In Sec. IV we determine flows and fixed point structure for the renormalization group equations in some detail in the case of short and long range isotropic force fields and determine the scaling properties. Since the discussion for anisotropic force fields is quite analogous we summarize this case in the Appendix. We conclude the paper with a summary and a conclusion in Sec V. A range of technical issues are for the record deferred to an extensive Appendix.

## II. THE MODEL

It is our aim to analyze the scaling properties of Lévy flights in a quenched random force field. For that purpose let us first discuss and summarize the properties of Lévy flights in a pure environment.

### A. Lévy flights

We consider a particle or for that matter a gas of non-interacting particles performing independent isotropic random motion in  $d$  dimensions. For the step size distribution we assume a normalized Lévy distribution [5,11,17,28–31]

$$p(\boldsymbol{\eta})d^d\eta = \frac{f\eta_0^f}{S_d}\eta^{-1-f}d\eta d\Omega \quad \text{and} \quad S_d = \frac{2\pi^{\frac{d}{2}}}{(d/2-1)!} . \quad (2.1)$$

Here  $\boldsymbol{\eta}$  is the microscopic step and the algebraic behavior in the large step regime is characterized by the microscopic step index  $f$ . In order to ensure normalization of the distribution  $p(\boldsymbol{\eta})$  we introduce a lower cut-off  $\eta_0$  of the order of a microscopic length and assume a positive step index,  $f > 0$ .  $S_d$  is the full solid angle on the surface of a unit sphere in  $d$  dimensions. In Fig. 1 we have depicted the Lévy distribution  $P(\boldsymbol{\eta})$ .

The macroscopic physics ensuing from the Lévy distribution for the microscopic elementary step depends entirely on the range characteristics of  $P(\boldsymbol{\eta})$ . For  $f > 2$  the second moment or mean square step,  $\langle \eta^2 \rangle = \int p(\boldsymbol{\eta})\eta^2 d^d\eta = \frac{f}{f-2}\eta_0^2$ , exists and a characteristic step size is given by the root mean square deviation  $\langle \eta^2 \rangle^{\frac{1}{2}}$ . For  $1 < f < 2$  the second

moment diverges, however, the mean step  $\langle \eta \rangle = \int p(\boldsymbol{\eta}) \eta d^d \eta = \frac{f}{f-1} \eta_0$  is finite, defining an effective step size. In the interval  $0 < f < 1$  the first moment diverges and even a mean step size is not defined.

For a Lévy flight consisting of  $N$  steps the end-to-end distance of the random walk is  $\mathbf{r}_N = \sum_{i=1}^N \boldsymbol{\eta}_i$  or, assuming one step per unit time,  $t = N$ ,  $\mathbf{r}(t) = \sum_{i=1}^t \boldsymbol{\eta}_i$ , and it follows generally that the mean square displacement for statistically independent step events is given by

$$\langle r^2(t) \rangle = t \langle \eta^2 \rangle . \quad (2.2)$$

Consequently, for general step distributions with a finite second moment or mean square step, as in particular the case for Lévy distribution for  $f > 2$ , the mean square displacement is proportional to the elapsed time. This behavior is characteristic of ordinary Brownian motion leading to diffusive behavior for a gas of Brownian walker and corresponds to the dynamic exponent  $z = 2$  in Eq. (1.1) [5,32].

On the other hand, for Lévy flight with step index  $f < 2$  the second moment  $\langle \eta^2 \rangle$  diverges, Eq.(2.2) is undefined and we cannot define a mean square displacement and a dynamic exponent  $z$  according to the heuristic definition in Eq. (1.1). However, this point will be clarified below. in terms of the probability distribution.

The probability distribution for the random walker is given by  $P(\mathbf{r}, t) = \langle \delta(\mathbf{r} - \mathbf{r}(t)) \rangle$  and is easily derived by means of the method of characteristic functions [5,17,30]. We obtain, noting that  $t$  is discrete,

$$P(\mathbf{r}, t) = \int e^{i\mathbf{k} \cdot \mathbf{r}} [p(\mathbf{k})]^t \frac{d^d k}{(2\pi)^d} , \quad (2.3)$$

where  $p(\mathbf{k})$  is the Fourier transform of the step distribution  $p(\boldsymbol{\eta})$ ,  $p(\mathbf{k}) = \int e^{-i\mathbf{k} \cdot \boldsymbol{\eta}} p(\boldsymbol{\eta}) d^d \eta$ . At large  $\mathbf{r}$  Eq. (2.3) samples the small  $\mathbf{k}$  region. For small  $\mathbf{k}$  the behavior of  $p(\mathbf{k})$  is controlled by the algebraic power law tail of  $p(\boldsymbol{\eta})$ . We find

$$p(\mathbf{k}) = 1 - D(k\eta_0)^\mu \simeq \exp[-D\eta_0^\mu k^\mu] , \quad (2.4)$$

where  $D$  is a dimensionless geometrical factor and  $\mu$  is a scaling index. For  $f > 2$  the second moment  $\langle \eta^2 \rangle$  exists and  $\mu$  locks onto 2; for  $f < 2$ ,  $\langle \eta^2 \rangle$  diverges and  $\mu = f$ . By insertion we obtain

$$P(\mathbf{r}, t) = \int \exp[i\mathbf{k} \cdot \mathbf{r} - |t| D\eta_0^\mu k^\mu] \frac{d^d k}{(2\pi)^d} . \quad (2.5)$$

In Fig. 2 we have shown the dependence of the scaling index  $\mu$  on the step index  $f$ . From the structure of Eq. (2.5) we infer that  $P(\mathbf{r}, t)$  has the scaling form

$$P(\mathbf{r}, t) = |t|^{-\frac{d}{\mu}} G(r/|t|^{\frac{1}{\mu}}) . \quad (2.6)$$

For  $f > 2$ ,  $\mu = 2$  and the scaling function  $G(x)$  takes a Gaussian form characteristic of ordinary Brownian motion,  $G(x) \simeq \exp(\text{const.} x^2)$ . This is a consequence of the central limit theorem [5] which here implies a universal behavior characterized by the exponent  $\mu = 2$ . For  $f < 2$ ,  $\mu = f$  and the scaling function  $G(x)$  can in general not be given explicitly in terms of known functions. For  $\mu = 1$ , the ballistic case  $r \sim t$ , we find the Cauchy distribution  $G(x) \simeq (1 + \text{const.} x^2)^{-((d+1)/2)}$ . It is, moreover, easy to show that  $G(x) \rightarrow \text{const.}$  for  $x \rightarrow 0$  and  $G(x) \rightarrow 0$  for  $x \rightarrow \infty$ .

The scaling properties of Lévy flights are described by Eqs. (2.5) and (2.6). From Eq. (2.6) we infer the mean square displacement  $\langle r^2(t) \rangle \sim t^{2/\mu}$ , i.e., according to Eq. (1.1) the dynamic exponent  $z = \mu$ , indicating superdiffusive behavior. However, as mentioned above this reasoning is not correct for Lévy flights. The expression in Eq. (2.2) is not defined for Lévy flights since  $\langle \eta^2 \rangle$  diverges and the scaling regime must be defined with some care if we wish to give meaning to Eq. (1.1). One way is to confine the Lévy flights to a volume of linear size  $L$ ; the mean square displacement is then given by  $\langle r^2(t) \rangle_L = \int_V r^2 P(\mathbf{r}, t) d^d r$ , where  $V = L^d$ . Using the scaling form in Eq. (2.6) with

$$G(r) = \left( \frac{1}{D^{1/\mu} \eta_0} \right)^d \int \exp[i\mathbf{k} \cdot \mathbf{r} / (D^{1/\mu} \eta_0) - k^\mu] \frac{d^d k}{(2\pi)^d} , \quad (2.7)$$

we obtain, changing variables, the mean square displacement

$$\langle r^2(t) \rangle_L = |t|^{2/\mu} \int_{(L/|t|^{1/\mu})^d} r^2 G(r) d^d r . \quad (2.8)$$

From Eq. (2.6) and (2.8) we infer that the characteristic time in the problem is the time  $\sim L^\mu$  it takes the random walker to traverse the volume  $V \sim L^d$ . At long times, i.e., for  $t^{1/\mu} \gg L$ ,

$$\langle r^2(t) \rangle_L = |t|^{2/\mu} \int_0^L r^2 G(r) d^d r = \text{const.} |t|^{2/\mu} \quad (2.9)$$

and comparing with Eq. (1.1) we deduce the dynamic exponent  $z = \mu$ . At short times,  $t^{1/\mu} \ll L$ , using  $G(r) \sim r^{-\mu-d}$  for  $r$  large, we obtain

$$\langle r^2(t) \rangle_L = \text{const.} |t| L^{2-\mu}, \quad (2.10)$$

in accordance with Eq. (2.2). For Lévy flights with  $\mu < 2$   $\langle r^2(t) \rangle_L$  diverges for  $t \rightarrow \infty$ . In the Brownian case  $\mu = 2$  and  $\langle r^2(t) \rangle \propto |t|$  in both cases in accordance with Eq. (2.2). Summarizing, in order to characterize anomalous superdiffusion arising from Lévy flights by means of the mean square displacement we must conceptually confine the flights to a box of size  $L$  and define the scaling region for  $t \gg L^\mu$ . Alternatively, we can discuss the scaling properties and the identification of  $z$  by means of the scaling form in Eq. (2.6) where the argument  $r$  controls the range in question.

### B. Langevin equation for Lévy flights

It is convenient to discuss Lévy flights in terms of a Langevin equation with “power law” noise [32,33]. In an arbitrary force field  $\mathbf{F}(\mathbf{r})$ , representing the quenched disordered environment, the equation takes the form

$$\frac{d\mathbf{r}(t)}{dt} = \mathbf{F}(\mathbf{r}(t)) + \boldsymbol{\eta}(t). \quad (2.11)$$

Here  $\boldsymbol{\eta}(t)$  is the instantly correlated power law white noise with the isotropic distribution given in Eq. (2.1) at a particular time instant.

The microscopic steps  $\boldsymbol{\eta}_i$  with distribution  $p(\boldsymbol{\eta}_i)$  constituting a Lévy flight are discrete processes, so properly speaking the Langevin equation (2.11) is the continuum limit of the corresponding difference equation defined for a discrete time step  $\Delta$ . This limit is singular and it is instructive to discuss the limiting procedure in some detail.

Limiting our discussion to the force-free case,  $\mathbf{F} = \mathbf{0}$ , setting  $\mathbf{r}_n = \mathbf{r}(t_n)$ ,  $\boldsymbol{\eta}_n = \boldsymbol{\eta}(t_n)$ , and  $t_n = n\Delta$ , the difference equation is given by  $(\mathbf{r}_{n+1} - \mathbf{r}_n)/\Delta = \boldsymbol{\eta}_n$  with solution  $\mathbf{r}_n = \Delta \sum_{p=0}^n \boldsymbol{\eta}_p$ . From the definition of  $P(\mathbf{r}, n) = \langle \delta(\mathbf{r} - \mathbf{r}_n) \rangle$ , we obtain, using  $\delta(\mathbf{r}) = \int \exp(-i\mathbf{k} \cdot \mathbf{r}) d^d k / (2\pi)^d$  together with  $\exp(i\mathbf{k} \cdot \mathbf{r}_n) = \prod_{p=0}^n \exp(i\Delta \mathbf{k} \cdot \boldsymbol{\eta}_p)$  for  $P(\mathbf{k}, n) = \int \exp(i\mathbf{k} \cdot \mathbf{r}) P(\mathbf{r}, n) d^d r$ ,

$$P(\mathbf{k}, n) = \langle \exp(i\Delta \mathbf{k} \cdot \boldsymbol{\eta}) \rangle^n \quad (2.12)$$

and the issue is to define the continuum limit  $\Delta \rightarrow 0$ , keeping  $t = n\Delta$  fixed, of the expression for  $P(\mathbf{k}, n)$  in Eq. (2.12). For simplicity we first consider the case of a Gaussian distribution for  $p(\boldsymbol{\eta})$ , i.e., the case of ordinary Brownian motion,  $p(\boldsymbol{\eta}) = (1/2\sigma\pi^{1/2})^d \exp(-\eta^2/4\sigma^2)$  of width  $2\sigma$ . Evaluating  $\langle \exp(i\Delta \mathbf{k} \cdot \boldsymbol{\eta}) \rangle$  by completing the square in the exponent we obtain  $P(\mathbf{k}, n) = \exp(-\Delta^2 \sigma^2 k^2 n)$ . In the continuum limit  $\Delta \sigma^2 \rightarrow D$  and we have the Gaussian distribution

$$P(\mathbf{k}, t) = \exp[-Dk^2 t]. \quad (2.13)$$

Correspondingly, the white noise condition, i.e., uncorrelated noise,  $\langle \eta_n^\alpha \eta_m^\beta \rangle = \sigma^2 \delta_{nm} \delta_{\alpha\beta}$ , becomes in the continuum limit

$$\langle \eta^\alpha(t) \eta^\beta(t') \rangle = D \delta^{\alpha\beta} \delta(t - t'). \quad (2.14)$$

Consequently, in the Gaussian case we must in the continuum limit  $\Delta \rightarrow 0$  scale the width  $\sigma$  of the noise distribution to infinity in order to obtain a finite diffusion coefficient  $D = \sigma^2 \Delta$ . In the Lévy case the noise distribution  $p(\boldsymbol{\eta})$  is given by Eq. (2.1) and from Eq.(2.4),  $\langle \exp(i\Delta \mathbf{k} \cdot \boldsymbol{\eta}) \rangle = 1 - D(k\Delta\eta_0)^f$  for  $f < 2$  and  $k\Delta\eta_0 \ll 1$ , i.e.,  $P(\mathbf{k}, n) = [1 - D(k\Delta\eta_0)^f]^n$ . Using the relation,  $(1 - x/n)^n \rightarrow \exp(-x)$  for  $n \rightarrow \infty$ , we obtain in the continuum limit  $\Delta \rightarrow 0$  and  $t = n\Delta$  fixed,

$$P(\mathbf{k}, t) = \exp[-D\eta_0^f \Delta^{f-1} k^f t]. \quad (2.15)$$

In order to eliminate the discrete time step  $\Delta$  and keep the coefficient  $D$  fixed we must renormalize the cut off  $\eta_0$  in the Lévy distribution (2.1) according to  $\eta_0^f \Delta^{f-1} = 1$ . We notice that the border line case is  $f = 1$ . For  $1 < f < 2$   $\eta_0 \rightarrow \infty$  for  $\Delta \rightarrow 0$ , i.e., the cut-off moves out to infinity. For  $0 < f < 1$ , on the other hand,  $\eta_0 \rightarrow 0$  for  $\Delta \rightarrow 0$ . We also notice that  $\Delta\eta_0 \rightarrow 0$  so that  $k\Delta\eta_0 \ll 1$  is satisfied for all  $f$ .

Summarizing, we can without loss of generality discuss Lévy flights (and Brownian motion) in terms of a continuous Langevin equation provided we scale the underlying discrete noise distributions accordingly. Note, however, that these renormalizations are not observable, the problem at hand is defined by the Langevin equations (2.11).

Lévy flights in an arbitrary force field are in principle described by the Langevin equation (2.11) together with the distribution in Eq. (2.1) for the noise  $\boldsymbol{\eta}$ . For a given force field the only random aspect resides in the noise  $\boldsymbol{\eta}$  which drives the position  $\mathbf{r}$  of the random walker; the force field  $\mathbf{F}(\mathbf{r})$  acts as a static background. However, for a random force field modelling the quenched static environment the Langevin equation (2.11) harbours two different kinds of stochasticity and it is convenient to recast the problem in terms of an associated Fokker-Planck equation, thereby absorbing the fluctuating Lévy noise  $\boldsymbol{\eta}(t)$ .

### C. Fokker-Planck equation for Lévy flights

In the absence of the force field, i.e.,  $\mathbf{F}(\mathbf{r}) = \mathbf{0}$ , it follows from Eq. (2.5) that  $P(\mathbf{k}, t)$  satisfies the equation

$$\frac{\partial P(\mathbf{k}, t)}{\partial t} = -D_1 k^\mu P(\mathbf{k}, t), \quad (2.16)$$

where we have absorbed the renormalized cut-off  $\eta_0$  in the Lévy coefficient  $D_1 = D\eta_0^\mu$ . The form of Eq. (2.16) leads us to suggest the following Fokker-Planck equation for a Lévy walker in a force field:

$$\frac{\partial P(\mathbf{r}, t)}{\partial t} = -\boldsymbol{\nabla} \cdot (\mathbf{F}(\mathbf{r})P(\mathbf{r}, t)) + D_1 \nabla^\mu P(\mathbf{r}, t) + D_2 \nabla^2 P(\mathbf{r}, t). \quad (2.17)$$

Here the first term on the right hand side of Eq. (2.17) is the usual drift term due to the motion of the walker in the force field, the second term arises from Eq. (2.16) where we have introduced the “fractional gradient operator”  $\nabla^\mu$  as the Fourier transform of  $-k^\mu$ .  $\nabla^\mu \sim r^{-d-\mu}$  is a spatially nonlocal integral operator reflecting the long range character of the Lévy steps; for  $\mu = 2$  it reduces to the usual Laplace operator describing ordinary diffusion [34]. Finally, we have for later purposes included the ordinary diffusion term,  $D_2 \nabla^2 P(\mathbf{r}, t)$ , originating from the next to leading long range part of the distribution  $p(\boldsymbol{\eta})$  and corresponding to the next leading term of order  $k^2$  in the expansion in Eq. (2.4). The derivation of the Fokker-Planck equation is discussed in more detail in Appendix A.

For the quenched random force field we assume a Gaussian distribution,

$$p(\mathbf{F}(\mathbf{r})) \propto \exp \left[ -\frac{1}{2} \int d^d r d^d r' F^\alpha(\mathbf{r}) \Delta^{\alpha\beta}(\mathbf{r} - \mathbf{r}')^{-1} F^\beta(\mathbf{r}') \right], \quad (2.18)$$

with the spatial correlations given by

$$\langle F^\alpha(\mathbf{r}) F^\beta(\mathbf{r}') \rangle_F = \Delta^{\alpha\beta}(\mathbf{r} - \mathbf{r}'). \quad (2.19)$$

Here  $\Delta^{\alpha\beta}(\mathbf{r} - \mathbf{r}')$  is the force correlation function expressing the range and vector character of  $\mathbf{F}(\mathbf{r})$  and  $\langle \dots \rangle_F$  denotes an average over the force field according to the distribution (2.18).

In the unconstrained case  $\Delta^{\alpha\beta}$  is diagonal; however, generally the force field breaks up into a longitudinal curl-free part  $\mathbf{E}$  and a transverse divergence-free part  $\mathbf{B}$ , i.e.,  $\mathbf{F} = \mathbf{E} + \mathbf{B}$ , where  $\boldsymbol{\nabla} \cdot \mathbf{B} = 0$  and  $\boldsymbol{\nabla} \times \mathbf{E} = \mathbf{0}$  [4,26,35]. Assuming that the cross correlation of  $\mathbf{E}$  and  $\mathbf{B}$  vanishes,  $\langle E^\alpha B^\beta \rangle = 0$ , we have in Fourier space

$$\langle E^\alpha(\mathbf{k}) E^\beta(\mathbf{k}') \rangle_F = (2\pi)^d \delta(\mathbf{k} + \mathbf{k}') \left[ \frac{k^\alpha k^\beta}{k^2} \right] \Delta^L(\mathbf{k}) \quad (2.20)$$

$$\langle B^\alpha(\mathbf{k}) B^\beta(\mathbf{k}') \rangle_F = (2\pi)^d \delta(\mathbf{k} + \mathbf{k}') \left[ \delta^{\alpha\beta} - \frac{k^\alpha k^\beta}{k^2} \right] \Delta^T(\mathbf{k}). \quad (2.21)$$

The case of an unconstrained force field then corresponds to  $\Delta^L = \Delta^T = \Delta$  and we obtain the force correlation function

$$\langle F^\alpha(\mathbf{k}) F^\beta(\mathbf{k}') \rangle_F = (2\pi)^d \delta(\mathbf{k} + \mathbf{k}') \delta^{\alpha\beta} \Delta(\mathbf{k}). \quad (2.22)$$

The range of the force correlations is characterized by the functions  $\Delta^L(\mathbf{k})$  and  $\Delta^T(\mathbf{k})$ .

In the case of a *finite range*, e.g.,  $\Delta^{L,T}(\mathbf{r}) \propto \exp(-rk_0)/r^{d-2}$ , with range parameter  $1/k_0$  we have  $\Delta^{L,T}(\mathbf{k}) \propto 1/(k^2 + k_0^2)$ . In the long wavelength limit  $k \rightarrow 0$   $\Delta^{L,T}(\mathbf{k}) \rightarrow \text{const.}$ , corresponding to the *zero range* case  $\Delta^{L,T}(\mathbf{r}) \propto \delta(\mathbf{r})$ . For *infinite range* the force correlations are characterized by the exponent  $a$ ,  $\Delta^{L,T}(\mathbf{r}) \propto r^{-a}$ ,  $\Delta^{L,T}(\mathbf{k}) \propto k^{a-d}$ .

Summarizing, we characterize a general force field by the following expressions for the longitudinal and transverse force correlation functions:

$$\Delta^L(\mathbf{k}) = \Delta_1^L + \Delta_2^L k^{a_L-d} \quad (2.23)$$

$$\Delta^T(\mathbf{k}) = \Delta_1^T + \Delta_2^T k^{a_T-d} . \quad (2.24)$$

We have here for completion introduced two separate indices,  $a_L$  and  $a_T$ , for the power law behavior of the longitudinal and transverse correlations, respectively. For  $a_{L,T} > d$ ,  $\Delta^{L,T}(\mathbf{k}) \rightarrow \Delta_1^{L,T}$ , in the long wavelength limit and we effectively retrieve the zero range case; for  $a_{L,T} < d$ ,  $\Delta^{L,T}(\mathbf{k}) \rightarrow \Delta_2^{L,T} k^{a_{L,T}-d}$  and the specific long range behavior enters in the  $\mathbf{k} \rightarrow \mathbf{0}$  limit.

### III. RENORMALIZATION GROUP THEORY

The problem of analyzing the asymptotic long time scaling properties of Lévy flights in a random quenched force field has now been reduced to an analysis of the random Fokker-Planck equation (2.17), in conjunction with the force distribution in Eq. (2.18) and the force correlation functions in Eqs. (2.19-2.21). In particular we wish to evaluate the scaling behavior of the distribution  $P(\mathbf{r}, t)$  averaged with respect to the force field, i.e.,  $\langle P(\mathbf{r}, t) \rangle_F$ .

#### A. Perturbation theory

There are a variety of techniques available in order to treat the random Fokker-Planck equation (2.17). Applying the Martin-Siggia-Rose formalism in functional form [36–40] and using either the replica method [4] or an explicit causal time dependence [18,38,40], one can average over the quenched force field and construct an effective field theory. A more direct method, which we shall adhere to in the present discussion, amounts to an expansion of the Fokker-Planck equation (2.17) in powers of the force field and an average over products of  $\mathbf{F}(\mathbf{r})$  according to the distribution in Eq. (2.18).

Defining the Laplace-Fourier transform

$$P(\mathbf{k}, \omega) = \int d^3r dt \exp(i\omega t - i\mathbf{k} \cdot \mathbf{r}) P(\mathbf{r}, t) \theta(t) , \quad (3.1)$$

where  $\theta(t)$  is the step function, we obtain, introducing for later purposes the dimensionless coupling strengths  $\lambda_L$  and  $\lambda_T$  for the vertices coupling to  $\mathbf{E}$  and  $\mathbf{B}$ , respectively, the Fokker-Planck equation

$$P(\mathbf{k}, \omega) = G_0(\mathbf{k}, \omega) P_0(\mathbf{k}) + G_0(\mathbf{k}, \omega) \int \frac{d^d p}{(2\pi)^d} [(-i)\lambda_L \mathbf{k} \cdot \mathbf{E}(\mathbf{k} - \mathbf{p}) + (-i)\lambda_T \mathbf{k} \cdot \mathbf{B}(\mathbf{k} - \mathbf{p})] P(\mathbf{p}, \omega) \quad (3.2)$$

Here the force field is averaged according to Eqs. (2.20-2.21) for all pairwise contractions according to the Wick's theorem following from the Gaussian distribution in Eq. (2.18),  $P_0(\mathbf{k}) = P(\mathbf{k}, t = 0)$  is the initial distribution, and we have, moreover, introduced the unperturbed propagator or Green's function

$$G_0(\mathbf{k}, \omega) = \frac{1}{-i\omega + D_1 k^\mu + D_2 k^2} . \quad (3.3)$$

The integral equation (3.2) immediately lends itself to a direct expansion in powers of  $\mathbf{E}, \mathbf{B}$  or  $\lambda_L, \lambda_T$ . In order to discuss the various perturbative contributions it is convenient to represent Eq. (3.2) diagrammatically as done in Fig. 3 [4,26,41–44]. Here  $P(\mathbf{k}, \omega)$  is characterized by a solid bar,  $P_0(\mathbf{k})$  by a cross, the vertices  $-i\lambda_L$  and  $-i\lambda_T$  by dots, the force fields  $\mathbf{E}$  and  $\mathbf{B}$  by wiggly lines, and  $G_0(\mathbf{k}, \omega)$  by a directed arrow.

Hence, iterating Eq. (3.2) in powers of  $\lambda_L$  and  $\lambda_T$  and averaging over the force fields, keeping one component fixed, we identify perturbative corrections to 1) the self energy, 2) the vertex functions, and 3) the force correlation functions. Defining the self energy  $\Sigma(\mathbf{k}, \omega)$  by means of the Dyson equation,

$$G(\mathbf{k}, \omega) = G_0(\mathbf{k}, \omega) + G_0(\mathbf{k}, \omega) \Sigma(\mathbf{k}, \omega) G(\mathbf{k}, \omega) , \quad (3.4)$$

shown diagrammatically in Fig. 4, where the renormalized propagator is indicated by a solid directed line and the self energy by a circle, we derive the renormalized Fokker-Planck equation shown in Fig. 5,

$$P(\mathbf{k}, \omega) = G(\mathbf{k}, \omega) P_0(\mathbf{k}) + G(\mathbf{k}, \omega) \int \frac{d^d p}{(2\pi)^d} [(-i)\mathbf{\Lambda}_L(\mathbf{k}, \mathbf{p}, \omega) \cdot \mathbf{E}(\mathbf{k} - \mathbf{p}) + (-i)\mathbf{\Lambda}_T(\mathbf{k}, \mathbf{p}, \omega) \cdot \mathbf{B}(\mathbf{k} - \mathbf{p})] P(\mathbf{p}, \omega) . \quad (3.5)$$

Here  $\mathbf{\Lambda}_L(\mathbf{k}, \mathbf{p}, \omega)$  and  $\mathbf{\Lambda}_T(\mathbf{k}, \mathbf{p}, \omega)$ , depicted as circles in Fig. 5, are the renormalized vertex functions; to lowest order  $\mathbf{\Lambda}_{L,T}(\mathbf{k}, \mathbf{p}, \omega) = \lambda_{L,T} \mathbf{k}$ . In a similar manner we extract corrections to the force correlation function from the 4-point vertex function  $\Gamma(\mathbf{k}, \mathbf{p}, \mathbf{l}, \omega)$  in Fig. 6 and the contraction  $\int \Gamma(\mathbf{k}, \mathbf{k}, \mathbf{l}, \omega) G(\mathbf{k} - \mathbf{l}, \omega) d^d l / (2\pi)^d$ , also shown in Fig. 6. To lowest order  $\Gamma(\mathbf{k}, \mathbf{k}, \mathbf{l}, \omega) = -k^\alpha \Delta^{\alpha\beta}(l)(k-l)^\beta$ , summed over  $\alpha$  and  $\beta$ , where  $\Delta^{\alpha\beta}$  is the force correlation function defined in Eqs. (2.19-2.21). To second order in  $\lambda_L$  and  $\lambda_T$  or first order in  $\Delta^L$  and  $\Delta^T$ , corresponding to first loop order in the field theoretic formulation [18,36–40] we find diagrammatic contributions to  $\Sigma$ ,  $\mathbf{\Lambda}_{L,T}$ , and  $\Gamma$  shown in Fig. 7, Fig. 8, and Fig. 9, respectively.

Let us first discuss the self energy correction. Solving the Dyson equation (3.4) the self energy  $\Sigma(\mathbf{k}, \omega)$  enters in the renormalized propagator,

$$G(\mathbf{k}, \omega) = \frac{1}{-i\omega + D_1 k^\mu + D_2 k^2 - \Sigma(\mathbf{k}, \omega)} , \quad (3.6)$$

and directly determines the diffusional character of the random walker. In Appendix B we discuss in some detail the evaluation of  $\Sigma(\mathbf{k}, \omega)$  to leading order in  $k^2$  on the basis of the diagrams in Fig. 7.

In the case of an isotropic unconstrained zero range force correlation function,  $\lambda_L = \lambda_T = \lambda$  and  $\Delta^L(\mathbf{k}) = \Delta^T(\mathbf{k}) = \Delta$ , we have in particular

$$\Sigma(\mathbf{k}, \omega) = -\lambda^2 \Delta \int \frac{d^d p}{(2\pi)^d} \mathbf{k} \cdot (\mathbf{k}/2 + \mathbf{p}) G_0(\mathbf{k}/2 + \mathbf{p}, \omega) . \quad (3.7)$$

To leading order in  $k^2$  the static contribution,  $\Sigma(\mathbf{k}, 0)$ , given in Appendix B, only contributes to the ordinary diffusion term  $D_2 k^2$  in Eq. (3.6); there is no correction to the anomalous Lévy term  $D_1 k^\mu$ . We shall see later that this has a profound effect on the scaling properties of Lévy flights. For the correction to the diffusion coefficient  $D_2$  we then find, performing the integration over the solid angle,

$$\delta D_2 = \frac{1}{2} \lambda^2 \Delta \frac{S_d}{d(2\pi)^d} \int_0^\Lambda dp \frac{D_1(d-\mu)p^{\mu+d-1} + D_2(d-2)p^{d+1}}{[D_1 p^\mu + D_2 p^2]^2} , \quad (3.8)$$

where  $S_d$  is given in Eq. (2.1) and we have introduced a UV cut-off corresponding to a microscopic length of order  $1/\Lambda$ . In the long wavelength limit  $p \rightarrow 0$  the integrand in Eq. (3.8) is dominated by the leading Lévy term  $\sim p^\mu$  and simple power counting shows that the integral is convergent for  $d > \mu$  yielding a correction to  $D_2$ . For  $d < \mu$  the integral diverges in the infrared limit  $p \rightarrow 0$  and we need a renormalization group approach in order to disentangle the true asymptotic scaling behavior. We encounter here the first *critical dimension*  $d_{c2} = \mu$  characterizing the behavior of the ordinary diffusion coefficient  $D_2$ . In the Brownian case [18–20]  $\mu = 2$  and the critical dimension is 2.

In a similar way we can discuss the vertex correction  $\mathbf{\Lambda}(\mathbf{k}, \mathbf{p}, \omega)$  on the basis of the diagrams in Fig. 8 in the isotropic case. The vertex function  $\mathbf{\Lambda}$  describes the coupling of the random walker to the quenched force field. In Appendix B we discuss in detail the evaluation of  $\mathbf{\Lambda}$ . We obtain

$$\mathbf{\Lambda}(\mathbf{k}, \mathbf{p}, \omega) = \lambda \mathbf{k} - \lambda^3 \Delta \int \frac{d^d l}{(2\pi)^d} (\mathbf{k} - \mathbf{l}) \mathbf{k} \cdot (\mathbf{p} - \mathbf{l}) G_0(\mathbf{k} - \mathbf{l}, \omega) G_0(\mathbf{p} - \mathbf{l}, \omega) \quad (3.9)$$

from which we extract to leading order in  $k$  and for  $\omega = 0$  the perturbative correction to  $\lambda$ ,

$$\delta \lambda = -\lambda^3 \Delta \frac{S_d}{d(2\pi)^d} \int_0^\Lambda dp \frac{p^{d+1}}{[D_1 p^\mu + D_2 p^2]^2} . \quad (3.10)$$

Similarly to our discussion of the self energy, the integral in Eq. (3.10) is convergent for  $d > 2\mu - 2$ , whereas for  $d < 2\mu - 2$  the correction  $\delta \lambda$  diverges in the far infrared limit  $p \rightarrow 0$ . We note here the appearance of a second *critical dimension*  $d_{c1} = 2\mu - 2$ , characterizing the behavior of the vertex correction. In the Brownian case  $\mu = 2$  and both the vertex and self energy diverges for  $d < 2$ . We also note that for  $\mu = 2$  the first order correction to  $D_2$  actually vanishes for  $d = 2$  thus requiring an expansion to second order in  $\Delta$  (fourth order in  $\lambda$ ) or, equivalently, to two-loop order [18].

Finally, we discuss the correction to the force correlation function  $\Delta$  extracted from the contraction of the 4-point vertex function depicted in Figs. 6 and 9. From the results in Appendix B we deduce

$$\begin{aligned}
\Gamma(\mathbf{k}, \mathbf{p}, \mathbf{l}, \omega) &= -\mathbf{k} \cdot (\mathbf{p} - \mathbf{l}) \lambda^2 \Delta \\
&+ \lambda^4 \Delta^2 \int \frac{d^d n}{(2\pi)^d} \mathbf{k} \cdot (\mathbf{p} - \mathbf{n})(\mathbf{k} - \mathbf{n}) \cdot (\mathbf{p} - \mathbf{l}) G_0(\mathbf{k} - \mathbf{n}, \omega) G_0(\mathbf{p} - \mathbf{n}, \omega) \\
&+ \lambda^4 \Delta^2 \int \frac{d^d n}{(2\pi)^d} \mathbf{k} \cdot (\mathbf{p} - \mathbf{l})(\mathbf{k} - \mathbf{n}) \cdot (\mathbf{p} - \mathbf{l} + \mathbf{n}) G_0(\mathbf{k} - \mathbf{n}, \omega) G_0(\mathbf{p} - \mathbf{l} + \mathbf{n}, \omega)
\end{aligned} \tag{3.11}$$

and we obtain, contracting Eq. (3.11), to leading order in  $k$  and for  $\omega = 0$  the perturbative correction to  $\Delta$ ,

$$\delta\Delta = \lambda^2 \Delta^2 \frac{S_d}{(2\pi)^d} \left(1 - \frac{1}{d}\right) \int_0^\Lambda dp \frac{p^{d+1}}{[D_1 p^\mu + D_2 p^2]^2} . \tag{3.12}$$

Also here we note that the correction to  $\Delta$  diverges for  $d < d_{c1}$ . In the Brownian case,  $\mu = 2$ , the critical dimensions coincide, i.e.,  $d_{c1} = d_{c2}$ .

## B. Momentum shell integration

In order to disentangle the breakdown of primitive perturbation theory and deduce the scaling properties of the force averaged distribution  $\langle P(\mathbf{r}, t) \rangle_F$  and the mean square displacement  $\langle \langle r^2(t) \rangle \rangle_F$  we carry out a dynamic renormalization group analysis, following the momentum shell integration method [26, 41, 43, 45]. This approach is a way of systematically diluting the short wavelength degrees of freedom, keeping the long wavelength modes controlling the asymptotic scaling behavior. The method derives from Wilson's original momentum space procedure [46] applied to static critical phenomena [42] and is an implementation of the real space Kadanoff construction in momentum space [43]. The application of renormalization group theory to dynamic phenomena described by Langevin-type equations was initiated in the context of dynamical critical phenomena in refs. [42, 48]. The implementation of the momentum shell integration method was introduced and discussed in refs. [41–43].

Here we briefly review the momentum shell integration method in the context of the Fokker-Planck equation (3.2), which in the case of an isotropic force field is expressed in the symbolic form

$$P = G_0 P_0 + \lambda G_0 F P . \tag{3.13}$$

Setting the UV cut-off  $\Lambda = 1$ , dividing the wave number interval  $0 < k < 1$  into a long wavelength regime  $0 < k < e^{-\ell}$ ,  $\ell > 0$ , including the long distance scaling region, and a short wavelength “shell” region  $e^{-\ell} < k < 1$ , the idea is now to average out the short wavelength degrees of freedom, using the distribution of the force field in Eqs. (2.18–2.19) in the shell  $e^{-\ell} < k < 1$ , in order to derive a renormalized Fokker-Planck equation valid for long wavelengths  $0 < k < e^{-\ell}$ . Projecting the Fokker-Planck equation (3.13) onto the two regions in wave number space we obtain the coupled equation

$$P' = G'_0 P'_0 + \lambda G'_0 (F P + F' P + F P' + F' P') \tag{3.14}$$

$$P = G_0 P_0 + \lambda G_0 (F P + F' P + F P' + F' P') , \tag{3.15}$$

where the prime refers to the shell  $e^{-\ell} < k < 1$ . Averaging the “long wavelength” Fokker-Planck equation (3.15) with respect to the short wavelength degrees of freedom in the shell we have, noting that  $\langle F' \rangle_{F'} = 0$ ,

$$\langle P \rangle_{F'} = G_0 P_0 + \lambda G_0 F P + \lambda G_0 F \langle P' \rangle_{F'} + \lambda G_0 \langle F' P' \rangle_{F'} . \tag{3.16}$$

The evaluation of  $\langle P' \rangle_{F'}$  and  $\langle F' P' \rangle_{F'}$  to a given order in  $\lambda$  is now achieved by expanding the “short wavelength” Fokker-Planck equation (3.14) and averaging over  $F'$ . Using that  $G_0 F G'_0$  and  $G_0 F' G'_0 F' G'_0$  vanish in the long wavelength limit, since two small wave numbers cannot add up to a wave number in the shell, and defining the force contraction according to the notation  $F'_{c_i} F'_{c_j} = \langle F' F' \rangle \delta_{ij}$ , we obtain

$$\begin{aligned}
\langle P \rangle_{F'} &= G_0 P_0 + \lambda G_0 F \langle P \rangle_{F'} + \lambda^2 G_0 F'_{c_1} G'_0 F'_{c_2} \langle P \rangle_{F'} + \lambda^4 G_0 F'_{c_1} G'_0 F'_{c_2} G'_0 F'_{c_1} G'_0 F'_{c_2} \langle P \rangle_{F'} \\
&+ \lambda^4 G_0 F'_{c_1} G'_0 F'_{c_2} G'_0 F'_{c_2} G'_0 F'_{c_1} \langle P \rangle_{F'} + \lambda^3 G_0 F'_{c_1} G'_0 F G'_0 F'_{c_2} \langle P \rangle_{F'} + \lambda^4 G_0 F'_{c_1} G'_0 F G'_0 F G'_0 F'_{c_2} \langle P \rangle_{F'}
\end{aligned} \tag{3.17}$$

which is diagrammatically depicted in Fig. 10.

We note that the momentum shell integration method combined with a perturbative expansion is essentially a nonlinear procedure leading to a more general Fokker-Planck equation involving higher order force fields as shown in Fig. 10 where the last diagram corresponds to two force fields  $F$  coupling to the distribution  $P$ . More importantly for deriving renormalization group equations we identify the same self energy, vertex, and force corrections as in primitive perturbation theory but now evaluated within the short wavelength shell. In this manner the elimination of the short wavelength degrees of freedom enters in the Fokker-Planck equation for the remaining long wavelength degrees of freedom.



### C. Renormalization group equations

While the general expression to first loop order for the self energy, vertex, and force correlation corrections and the general renormalization group equations are given in Appendix B, we here present a detailed derivation of the renormalization group equations in the isotropic short range case.

Disregarding the two-force term in Eq. (3.17) which is of higher order in  $k$  and therefore becomes irrelevant in the long wavelength limit, we obtain the renormalized Fokker-Planck equation

$$[-i\omega + D_1 k^\mu + (D_2 + \delta D_2) k^2] P(\mathbf{k}, \omega) = P_0(\mathbf{k}) + (\lambda + \delta\lambda) \int \frac{d^d p}{(2\pi)^d} (-i) \mathbf{k} \cdot \mathbf{F}(\mathbf{k} - \mathbf{p}) P(\mathbf{p}, \omega) \quad (3.18)$$

and force correlation function

$$\langle F^\alpha(\mathbf{k}) F^\beta(\mathbf{p}) \rangle_F = (\Delta + \delta\Delta) \delta^{\alpha\beta} (2\pi)^d \delta(\mathbf{k} + \mathbf{p}) , \quad (3.19)$$

both valid for wave numbers in the interval for  $0 < k, p < e^{-\ell}$ .

The first step in deriving renormalization group equations is then to rescale the wave number range to  $0 < k, p < 1$  and in this manner compensate for the eliminated degrees of freedom. Rescaling at the same time frequency, probability distribution, and force field, according to

$$\mathbf{k}' = \mathbf{k} e^\ell \quad (3.20)$$

$$\omega' = \omega e^{\alpha(\ell)} \quad (3.21)$$

$$P'(\mathbf{k}', \omega') = P(\mathbf{k}, \omega) e^{-\alpha(\ell)} \quad (3.22)$$

$$\mathbf{F}'(\mathbf{k}') = \mathbf{F}(\mathbf{k}) e^{-\beta(\ell)} , \quad (3.23)$$

where  $\alpha(\ell)$  and  $\beta(\ell)$  are to be determined subsequently, we thus obtain the renormalized Fokker-Planck equation

$$[-i\omega' + D'_1(\ell) k'^\mu + D'_2(\ell) k'^2] P'(\mathbf{k}', \omega') = P'_0(\mathbf{k}') + (-i) \lambda'(\ell) \int \frac{d^d p'}{(2\pi)^d} \mathbf{k}' \cdot \mathbf{F}'(\mathbf{k}' - \mathbf{p}') P'(\mathbf{p}', \omega') \quad (3.24)$$

and force correlation function

$$\langle F^{\alpha'}(\mathbf{k}') F^{\beta'}(\mathbf{p}') \rangle_{F'} = \Delta'(\ell) \delta^{\alpha'\beta'} (2\pi)^d \delta(\mathbf{k}' + \mathbf{p}') . \quad (3.25)$$

for wave numbers  $k'$  and  $p'$  in the original range  $0 < k', p' < 1$ ; note that  $P_0(\mathbf{k}) = P'_0(\mathbf{k}')$ . We have here introduced the scale dependent parameters  $D'_1(\ell)$ ,  $D'_2(\ell)$ ,  $\lambda'(\ell)$ , and  $\Delta'(\ell)$  given by

$$D'_1(\ell) = D_1 e^{-\ell\mu + \alpha(\ell)} \quad (3.26)$$

$$D'_2(\ell) = (D_2 + \delta D_2(\ell)) e^{-2\ell + \alpha(\ell)} \quad (3.27)$$

$$\lambda'(\ell) = (\lambda + \delta\lambda(\ell)) e^{-\ell(1+d) + \alpha(\ell) + \beta(\ell)} \quad (3.28)$$

$$\Delta'(\ell) = (\Delta + \delta\Delta(\ell)) e^{d\ell - 2\beta(\ell)} . \quad (3.29)$$

Note that the corrections  $\delta D_2(\ell)$ ,  $\delta\lambda(\ell)$ , and  $\delta\Delta(\ell)$  depend on the scale parameter  $\ell$  since they are evaluated in the short wavelength shell  $e^{-\ell} < k < 1$ .

In order to allow for an iteration the renormalization group equations are recast in differential form by considering an infinitesimal scale parameter  $\ell$  and expanding the right hand sides of Eqs. (3.26-3.29). Defining

$$\alpha(\ell) = \int_0^\ell z(e') d\ell' \quad (3.30)$$

$$\beta(\ell) = \int_0^\ell u(\ell') d\ell' \quad (3.31)$$

and noting from Eqs. (3.8), (3.10), and (3.12) evaluated on the shell  $k, p = 1$  that

$$\delta D_2 \propto \frac{1}{2} \frac{S_d}{(2\pi)^d} \frac{1}{d} \frac{D_1(d - \mu) + D_2(d - 2)}{[D_1 + D_2]^2} \lambda^2 \Delta \ell \quad (3.32)$$

$$\delta\lambda \propto -\frac{S_d}{(2\pi)^d} \frac{1}{d} \frac{\lambda^3 \Delta}{[D_1 + D_2]^2} \ell \quad (3.33)$$

$$\delta\Delta \propto \frac{S_d}{(2\pi)^d} \left(1 - \frac{1}{d}\right) \frac{\lambda^2 \Delta}{[D_1 + D_2]^2} \ell . \quad (3.34)$$

We arrive at the differential renormalization group equations

$$\frac{dD_1}{d\ell} = (z - \mu)D_1 \quad (3.35)$$

$$\frac{dD_2}{d\ell} = (z - 2)D_2 + A \frac{D_1(d - \mu) + D_2(d - 2)}{[D_1 + D_2]^2} \lambda^2 \Delta \quad (3.36)$$

$$\frac{d\lambda}{d\ell} = (z + u - 1 - d)\lambda - 2A \frac{\lambda^3 \Delta}{[D_1 + D_2]^2} \quad (3.37)$$

$$\frac{d\Delta}{d\ell} = (d - 2u)\Delta + 2A(d - 1) \frac{\lambda^2 \Delta}{[D_1 + D_2]^2}, \quad (3.38)$$

where  $A = (1/2d)S_d/(2\pi)^d$  is a geometrical factor,  $S_d = 2\pi^{d/2}/(d/2 - 1)!$  (cf. Eq. (2.1)).

In conformity with Ref. [26] we have included a vertex coupling  $\lambda$ . However, since  $\lambda^2$  is always associated with  $\Delta$  in the diagrammatic expansion, the inclusion of both  $\lambda$  and  $\Delta$  is essentially superfluous and we can for example set  $\lambda = 1$  and discuss the coupling to the force field by means of  $\Delta$  alone [18]. Thus assuming  $d\lambda(\ell)/d\ell = 0$  in Eq. (3.37) and solving for  $u(\ell)$  we finally obtain the renormalization group equations

$$\frac{dD_1}{d\ell} = (z - \mu)D_1 \quad (3.39)$$

$$\frac{dD_2}{d\ell} = (z - 2)D_2 + A \frac{D_1(d - \mu) + D_2(d - 2)}{[D_1 + D_2]^2} \Delta \quad (3.40)$$

$$\frac{d\Delta}{d\ell} = (2z - d - 2)\Delta - 2A(3 - d) \frac{\Delta^2}{[D_1 + D_2]^2} \quad (3.41)$$

which provides the basis for the discussion of the scaling properties of Lévy flights in an isotropic short range force field.

Deferring details to Appendices B and C we obtain in a precisely analogous manner the renormalization group equations for  $D_1$ ,  $D_2$ ,  $\Delta_1^L$ ,  $\Delta_2^L$ ,  $\Delta_1^T$ , and  $\Delta_2^T$ , in the case of Lévy flights in a general force field with range characterized by the indices  $a_L$  and  $a_T$ :

$$\frac{dD_1}{d\ell} = (z - \mu)D_1 \quad (3.42)$$

$$\begin{aligned} \frac{dD_2}{d\ell} = & (z - 2)D_2 \\ & + A \frac{(\Delta_1^L + \Delta_2^L)(D_1(2 - \mu - d) + D_2(-d))}{[D_1 + D_2]^2} \\ & + A \frac{(\Delta_1^T + \Delta_2^T)(D_1(2d - 2) + D_2(2d - 2))}{[D_1 + D_2]^2} \\ & + A \frac{\Delta_2^L(d - a_L)(D_1 + D_2)}{[D_1 + D_2]^2} \end{aligned} \quad (3.43)$$

$$\begin{aligned} \frac{d\Delta_1^L}{d\ell} = & (2z - d - 2)\Delta_1^L - 4A \frac{\Delta_1^L + \Delta_2^L}{[D_1 + D_2]^2} \Delta_1^L \\ & + A(2d - 2) \frac{(\Delta_1^T + \Delta_2^T)(\Delta_1^L + \Delta_2^L)}{[D_1 + D_2]^2} \end{aligned} \quad (3.44)$$

$$\begin{aligned} \frac{d\Delta_1^T}{d\ell} = & (2z - d - 2)\Delta_1^T - 4A \frac{\Delta_1^L + \Delta_2^L}{[D_1 + D_2]^2} \Delta_1^T \\ & + A(2d - 2) \frac{(\Delta_1^T + \Delta_2^T)(\Delta_1^L + \Delta_2^L)}{[D_1 + D_2]^2} \end{aligned} \quad (3.45)$$

$$\frac{d\Delta_2^L}{d\ell} = (2z - 2 - a_L)\Delta_2^L - 4A \frac{\Delta_1^L + \Delta_2^L}{[D_1 + D_2]^2} \Delta_2^L \quad (3.46)$$

$$\frac{d\Delta_2^T}{d\ell} = (2z - 2 - a_T)\Delta_2^T - 4A \frac{\Delta_1^L + \Delta_2^L}{[D_1 + D_2]^2} \Delta_2^T \quad (3.47)$$

## IV. DISCUSSION

We now turn to a discussion of the renormalization group equations derived in Sec. III. The Eqs. (3.39-3.41) describe the scaling properties in the isotropic short range case, whereas the Eqs. (3.42-3.47) account for the general case of anisotropic force fields with short or long range correlations. We discuss the isotropic short range and long range cases in some detail and summarize the results for the anisotropic cases, deferring details to the Appendix.

We notice immediately a general feature of the renormalization group equations (3.42-3.47): The requirement that the anomalous diffusion coefficient  $D_1$ , characterizing the amplitude of the Lévy term  $D_1 k^\mu$ , stays constant under renormalization, i.e.,  $dD_1(\ell)/d\ell = 0$  in Eq. (3.42), immediately implies that the dynamic scale dependent exponent  $z(\ell)$  locks onto the scaling index  $\mu$ , i.e.,

$$z = \mu . \quad (4.1)$$

Consequently, in the case of Lévy flights in a weak random force field the long time scaling behavior is entirely controlled by the leading anomalous Lévy term  $D_1 k^\mu$  and the dynamic exponent  $z$  locks onto  $\mu$ . In other words, the random force field has no influence on the Lévy flights. The intrinsic long range superdiffusive behavior, that is the occurrence of *rare events*, enables the walker to escape the inhomogeneous pinning environment and the long time behavior is the same as in the pure case. Below we substantiate this claim in more detail when we discuss the isotropic short range case.

### A. The isotropic short range case

In the case of an unconstrained short range force field the renormalization group equations are given by Eqs. (3.39-3.41). They describe how the parameters in the renormalized long wavelength Fokker-Planck equation (3.24) and force correlation function (3.25) change as we differentially average out the short wavelength degrees of freedom in the shell  $e^{-\ell} < k < 1$ , characterized by the scale parameter  $\ell$ .

#### 1. Renormalization group flow and fixed point structure

Requiring a constant anomalous diffusion coefficient  $D_1$  under renormalization, i.e.,  $dD_1(\ell)/d\ell = 0$ , Eq. (3.39) implies that the dynamic scale dependent exponent  $z(\ell)$  locks onto  $\mu$ ,  $z(\ell) = \mu$ , and we obtain the renormalization group equations for  $D_2$  and  $\Delta$ ,

$$\frac{dD_2}{d\ell} = (\mu - 2)D_2 + A \frac{D_1(d - \mu) + D_2(d - 2)}{[D_1 + D_2]^2} \Delta \quad (4.2)$$

$$\frac{d\Delta}{d\ell} = \epsilon \Delta - 2A(3 - d) \frac{\Delta^2}{[D_1 + D_2]^2} \quad (4.3)$$

$$\epsilon = d_{c1} - d \quad (4.4)$$

$$d_{c1} = 2\mu - 2 . \quad (4.5)$$

The Eqs. (4.2-4.3) determine the renormalization group flow in the  $D_2 - \Delta$  parameter space. We have introduced the parameter  $\epsilon$  and  $d_{c1}$  is the critical dimension. The Eqs. (4.2-4.3) determine the renormalization group flow in the  $D_2 - \Delta$  parameter space.

Above the critical dimension for  $\epsilon < 0$ , i.e.,  $d > d_{c1} = 2\mu - 2$  or  $\mu < 1 + d/2$ , Eqs. (4.2-4.3) have the trivial Gaussian fixed points  $D_2^* = 0$  and  $\Delta^* = 0$ , indicating that (i) the subleading diffusion term,  $D_2 k^2$ , scales to zero compared with the leading Lévy term and (ii) the quenched disorder, characterized by  $\Delta$ , scales to zero and thus is *irrelevant*. The effective long wavelength Fokker-Planck equation takes the form

$$(-i\omega + D_1 k^\mu)P(\mathbf{k}, \omega) = P_0(\mathbf{k}) \quad (4.6)$$

and for a particle at the origin at  $t = 0$ , i.e.,  $P_0(\mathbf{k}) = 1$ , we obtain the scaling expressions in Eqs. (2.5-2.6) with dynamic exponent  $z = \mu$ . Clearly, the physics is characterized by the interplay between the dimension  $d$  of configuration space and the index  $\mu$  specifying the tail of the Lévy distribution. For  $\mu < 1 + d/2$  the long range Lévy steps predominate and control the scaling behavior.

Below the critical dimension for  $\epsilon > 0$ , i.e.,  $d < d_{c1} = 2\mu - 2$ , or  $1 + d/2 < \mu < 2$ , we obtain, solving Eqs. (4.2-4.3) for  $dP_2/d\ell = 0$  and  $d\Delta/d\ell = 0$ , the non-trivial fixed point values for  $D_2$  and  $\Delta$ :

$$D_2^* = -D_1 \frac{(\mu - d)\epsilon}{(2 - \mu)(6 - 2d) + (2 - d)\epsilon} \quad (4.7)$$

$$\Delta^* = \epsilon \frac{(D_1 + D_2^*)^2}{2A(3 - d)} . \quad (4.8)$$

The fixed point  $D_2^*$  indicates that the subleading diffusive term  $D_2 k^2$  yields a contribution compared to the Lévy term  $D_1 k^\mu$ . The fixed point value of the diffusion coefficient  $D_2^*$  is negative since the pinning environment created by the random force field reduces the ordinary diffusion coefficient from its value  $D_2^* = 0$  for  $\mu < 1 + d/2$ . The emergence of the fixed point  $\Delta^*$  shows that for  $d$  less than the critical dimension  $d_{c1} = 2\mu - 2$  the quenched disorder in the long wavelength Fokker-Planck equation becomes *relevant*. In Fig. 11 we have shown the critical dimension  $d_{c1}$  as a function of the scaling index  $\mu$ . For  $\mu = 2$  we have the Brownian case  $d_{c1} = 2$ ; for  $d < \mu < 2$  the critical dimension  $d_{c1}$  depends linearly on  $\mu$ . Note that  $d_{c1} = 0$  in the ballistic case for  $\mu = 1$ . The line  $d = d_{c2} = \mu$  delimits the region  $d < d_{c2}$  where naive perturbation theory for  $\delta D_2$  diverges as discussed in Sec. III.

In the Brownian case  $\mu \rightarrow 2$  it follows from Eq. (4.7) that  $D_2^* \rightarrow -D_1$  so that the Lévy term  $D_1 k^\mu$  precisely cancels the diffusive term  $D_2 k^2$  in the Fokker-Planck equation (3.2); this is consistent with the fact that there is no correction to first loop order or more precisely to first order in  $\epsilon = d_{c1} - d$  in the Brownian case [18]. In Fig. 12 we have plotted the position of the fixed point  $(\Delta^*, D_2^*)$  as a function of the scaling index  $\mu$  for  $\epsilon = d_{c1} - d > 0$  or  $1 + d/2 < \mu < 2$ .

## 2. Scaling properties

Introducing the notation  $P(\mathbf{k}, \omega, D_1, D_2, \Delta) = \langle P(\mathbf{k}, \omega) \rangle_F$ , the scaling properties of  $\langle P(\mathbf{k}, \omega) \rangle_F$  are determined in the long wavelength limit by noting that  $\langle P(\mathbf{k}, \omega) \rangle_F$  can equally well be computed from the original Fokker-Planck equation (3.2) as from the renormalized equation (3.24). From the explicit scaling definitions in Eqs.(3.20-3.23) we thus obtain the homogeneity relation,

$$P(\mathbf{k}, \omega, D_1, D_2, \Delta) = e^{\alpha(\ell)} P(\mathbf{k}e^\ell, \omega e^{\alpha(\ell)}, D_1(\ell), D_2(\ell), \Delta(\ell)) \quad (4.9)$$

which determines how  $\langle P(\mathbf{k}, \omega) \rangle_F$  varies as we average out the short wavelength degrees of freedom parametrized by the scale parameter  $\ell$ . Similarly, we can derive a homogeneity relation for the wave number and frequency dependent diffusion coefficient  $D_2(\mathbf{k}, \omega, D_1, D_2, \Delta)$ , defined according to the Dyson equation (3.4) and  $k^2 D_2(\mathbf{k}, \omega) = -\Sigma(\mathbf{k}, \omega)$ . From Eq. (4.9) we thus obtain

$$D_2(\mathbf{k}, \omega, D_1, D_2, \Delta) = e^{2\ell - \alpha(\ell)} D_2(\mathbf{k}e^\ell, \omega e^{\alpha(\ell)}, D_1(\ell), D_2(\ell), \Delta(\ell)) . \quad (4.10)$$

In the vicinity of the fixed point  $(\Delta^*, D_2^*)$ , i.e., for large  $\ell$ , we have, setting from Eqs. (3.30) and (4.1)  $\alpha(\ell) = \mu\ell$  and choosing wave numbers  $\mathbf{k}$  such that  $\mathbf{k}e^\ell \sim 1$ , the scaling forms

$$P(\mathbf{k}, \omega, D_1, D_2, \Delta) = k^{-\mu} L(k/\omega^{1/\mu}, D_1, D_2^*, \Delta^*) \quad (4.11)$$

$$D_2(\mathbf{k}, \omega, D_1, D_2, \Delta) = k^{\mu-2} M(k/\omega^{1/\mu}, D_1, D_2^*, \Delta^*) , \quad (4.12)$$

where  $L$  and  $M$  are scaling functions. Making use of Eq. (3.1) we also have

$$P(\mathbf{r}, t, D_1, D_2, \Delta) = |t|^{-d/\mu} G(\mathbf{r}/|t|^{1/\mu}, D_1, D_2^*, \Delta^*) , \quad (4.13)$$

similar to the scaling form in Eq. (2.6) in the absence of the force field and we infer as in Sec. II a dynamic exponent  $z$  equal to the Lévy scaling index  $\mu$ , i.e.,  $z = \mu$ .

Above the critical dimension, i.e., for  $\epsilon < 0$  or  $d > d_{c1} = 2\mu - 2$ , we have the Gaussian fixed point  $(D_2^*, \Delta^*) = (0, 0)$  and we infer from Eq. (4.6) the complex scaling function

$$L(x, D_1, 0, 0) = \frac{ix^\mu}{iD_1 x^\mu + 1} . \quad (4.14)$$

### 3. Scaling relations and long time tails

Using the matching procedure [26,43,45] we can also derive scaling relations for the wave number frequency-dependent diffusion coefficient  $D_2(\mathbf{k}, \omega)$ . Expanding the renormalization group equations (4.2) and (4.3) to first order in  $\epsilon$  about the fixed point  $(\Delta^*, D_2^*)$  and defining  $\Delta(\ell) = \Delta^* + \delta\Delta(\ell)$  and  $D_2(\ell) = D_2^* + \delta D_2(\ell)$  the linearized equations take the form  $d\delta D_2/d\ell = -(2-\mu)\delta D_2 + A((d-\mu)/D_1)\delta\Delta$  and  $d\delta\Delta/d\ell = -|\epsilon|\delta\Delta$  with solutions

$$\delta D_2(\ell) = \left[ \delta D_2^0 + A \frac{\delta\Delta^0}{D_1} \right] e^{-(2-\mu)\ell} - A \frac{\delta\Delta^0}{D_1} e^{-|\epsilon|\ell} \quad (4.15)$$

$$\delta\Delta(\ell) = \delta\Delta^0 e^{-|\epsilon|\ell} . \quad (4.16)$$

Here  $\delta\Delta^0 = \delta\Delta(0)$  and  $\delta D_2^0 = \delta D_2(0)$  and Eqs. (4.15-4.16) hold both above and below the critical dimension  $d_{c1}$ . Since  $z(\ell)$  is locked on to  $\mu$  and suppressing the dependence on  $D_1$  we obtain from Eq. (4.10)

$$D_2(\mathbf{k}, \omega, D_2, \Delta) = e^{(2-\mu)\ell} D_2(\mathbf{k}e^\ell, \omega e^{\mu\ell}, D_2^* + \delta D_2(\ell), \Delta^* + \delta\Delta(\ell)) , \quad (4.17)$$

where  $\delta D_2(\ell)$  and  $\delta\Delta(\ell)$  are given by Eqs. (4.15-4.16).

In the long wavelength limit  $\mathbf{k} \rightarrow 0$  and choosing  $\ell$  such that  $\omega e^{\mu\ell} \simeq 1$  and from Appendix B,  $D_2(\mathbf{0}, 1, D_2, \Delta) \propto \Delta$ , we obtain, inserting Eq. (4.16), the scaling expression

$$D_2(\mathbf{0}, \omega, D_2, \Delta) \propto \omega^{-\frac{(2-\mu)}{\mu}} \left[ \Delta^* + \delta\Delta^0 \omega^{|\epsilon|/\mu} \right] . \quad (4.18)$$

Above the critical dimension, i.e., for  $d > d_{c1} = 2\mu - 2$  or  $\epsilon < 0$ ,  $\Delta^* = 0$  and we have

$$D_2(\mathbf{0}, \omega, D_2, \Delta) \propto \delta\Delta^0 \omega^{(d-d_{c2})/d_{c2}} , \quad (4.19)$$

where we have introduced the other critical dimension

$$d_{c2} = \mu . \quad (4.20)$$

In the low frequency limit  $\omega \rightarrow 0$  the coefficient  $D_2$  vanishes for  $d > d_{c2}$  and diverges for  $d_{c1} < d < d_{c2}$ . This behavior is consistent with our remarks in Sec. III and clarifies the nature of the divergence. In fact,  $d_{c2} = \mu$  plays the role of a second critical dimension controlling the behavior of the subleading diffusion coefficient  $D_2$  and supports the heuristic argument by Bouchaud et al. in [27]. In the Brownian case  $\mu = 2$  the two critical dimensions coincide.

Below the critical dimension,  $d < d_{c1}$  or  $\epsilon > 0$ ,  $\Delta^* > 0$  and we have the leading behavior

$$D_2(\mathbf{0}, \omega, D_2, \Delta) \propto \Delta^* \omega^{-(2-d_{c2})/d_{c2}} \quad (4.21)$$

which shows divergent behavior in the low frequency limit.

From  $D_2(t) = \int \exp(-i\omega t) D_2(\omega) d\omega / 2\pi$  we finally obtain the algebraic long time tails for the time dependent diffusion coefficient:

$$D_2(\mathbf{0}, t, D_2, \Delta) \propto t^{-d/d_{c2}} \quad \text{for } d > d_{c1} , \quad (4.22)$$

$$D_2(\mathbf{0}, t, D_2, \Delta) \propto t^{-d_{c1}/d_{c2}} \quad \text{for } d < d_{c1} . \quad (4.23)$$

In a similar way we can extract the behavior of  $D_2(\mathbf{k}, \omega, D_2, \Delta)$  in the long wavelength limit. Setting  $\omega = 0$  in Eq. (4.17) and choosing  $\ell$  such that  $\mathbf{k}e^\ell \simeq 1$  we obtain

$$D_2(\mathbf{k}, 0, D_2, \Delta) \propto k^{-(2-\mu)} \left[ \Delta^* + \delta\Delta^0 k^{|\epsilon|} \right] , \quad (4.24)$$

i.e.,

$$D_2(\mathbf{k}, 0, D_2, \Delta) \propto \delta\Delta^0 k^{d-d_{c2}} \quad \text{for } d > d_{c1} \quad (4.25)$$

$$D_2(\mathbf{k}, 0, D_2, \Delta) \propto \Delta^* k^{-(2-d_{c2})} \quad \text{for } d < d_{c1} . \quad (4.26)$$

For  $d > d_{c2}$   $D_2$  vanishes in the long wavelength limit  $\mathbf{k} \rightarrow 0$ ; for  $d < d_{c2}$   $D_2$  is divergent, in accordance with our previous discussion.

The spatial dependence is inferred from  $D_2(\mathbf{r}) = \int \exp(i\mathbf{k}\mathbf{r})D_2(\mathbf{k})d^d k/(2\pi)^d$  and we derive the algebraic long range fall-off

$$D_2(\mathbf{r}, 0, D_2, \Delta) \propto r^{d_{c2}-2d} \quad \text{for } d > d_{c1} \quad (4.27)$$

$$D_2(\mathbf{r}, 0, D_2, \Delta) \propto r^{2-d-d_{2c}} \quad \text{for } d < d_{c1} \quad (4.28)$$

In Fig. 11 the line  $d = d_{c2}$ , the second critical dimension, delimits the regions for the behavior of  $D_2$ . For  $d > d_{c2}$   $D_2$  converges, for  $d < d_{c2}$   $D_2$  is divergent.

It is instructive to consider the renormalization group flow in the  $\Delta - D_2$  plane about a fixed point in more detail. This discussion is carried out in Appendix D. Another issue, in the analysis of the renormalization group equations (3.38)-(3.40) we chose to keep the Lévy coefficient  $D_1$  fixed under a renormalization group transformation. This requirement leads, among other results, to  $z = \mu$  which is one of the main conclusions of the present work. Clearly, keeping  $D_1$  fixed is an arbitrary choice and our scaling results cannot depend on this choice. This point is discussed in Appendix E.

## B. The isotropic long range case

We now turn to a discussion of the case of Lévy flights in an isotropic long range random force field characterized by a fall-off exponent  $a$ . The case of Brownian motion in an algebraic long range field has been discussed by several authors [4,40,27,49–52] both to first and second loop order. The main conclusion here is that provided the force field falls off slowly enough the long range force correlations interfere with the Brownian walk and give rise to anomalous diffusion in any dimension. For comparison we have summarized the Brownian case in Appendix F.

Keeping as usual  $D_1$  fixed by locking  $z$  onto  $\mu$  we extract from the general equations (3.42-3.47) the appropriate renormalization group equations for  $D_2$  and  $\Delta_2 = \Delta$ ,

$$\frac{dD_2}{d\ell} = (\mu - 2)D_2 + A \frac{D_1(2d - \mu - a) + D_2(2d - 2 - a)}{[D_1 + D_2]^2} \Delta \quad (4.29)$$

$$\frac{d\Delta}{d\ell} = \epsilon\Delta - 4A \frac{\Delta^2}{[D_1 + D_2]^2}, \quad (4.30)$$

where we have introduced the expansion parameter

$$\epsilon = a_{c1} - a. \quad (4.31)$$

Here  $a_{c1} = 2\mu - 2$  has the same value as the critical dimension defined in Eq. (4.5) for the short range case. In the present context  $a_{c1}$ , of course, plays the role of a critical fall-off exponent for the long range force correlations.

The analysis now proceeds precisely as in the short range case. For  $\epsilon < 0$ , i.e.,  $a > a_{c1} = 2\mu - 2$  or  $\mu < 1 + a/2$ , we obtain the trivial Gaussian fixed points  $D_2^* = 0$ , and  $\Delta^* = 0$ , showing that (i) the subleading diffusion term  $D_2 k^2$  scales to zero compared with the leading Lévy term and (ii) the quenched disorder, characterized by  $\Delta$ , scales to zero and thus is *irrelevant*. The effective long wavelength Fokker-Planck equation takes the form in Eq. (4.6) and we obtain the scaling expressions in Eqs. (2.5-2.6) with dynamic exponent  $z = \mu$ . In contrast to the short range case, where the physics is controlled by the interplay between the dimension  $d$  of configuration place and the Lévy index  $\mu$ , the fall-off exponent  $a$  replaces  $d$  in the long range case for  $a < d$ . For  $a > a_{c1}$  or  $\mu < 1 + a/2$  the long range Lévy steps predominate and determine the scaling behavior.

For  $\epsilon > 0$ , i.e.,  $a < a_{c1}$  or  $\mu > 1 + a/2$ , we obtain the non-trivial fixed point values,  $D_2^* = -D_1(2d - \mu - a)\epsilon/(4(\mu - 2) + (2d - 2 - a)\epsilon)$  and  $\Delta^* = \epsilon(D_1 + D_2^*)^2/4A$ , indicating that the subleading term  $D_2 k^2$  yields a contribution compared to the Lévy term  $D_1 k^\mu$  and that the quenched disorder becomes *relevant*. In the Brownian case  $\mu \rightarrow 2$   $D_2^* \rightarrow -D_2$ , i.e., the Lévy term  $D_1 k^\mu$  precisely cancels the diffusive term  $D_2 k^2$  in the Fokker-Planck equation (3.2).

To leading order in  $\epsilon$  we have the fixed points  $(D_2^*, \Delta^*) = (0, 0)$  for  $\epsilon < 0$  and the fixed points,  $D_2^* = \epsilon[(2d - \mu - a)/4(2 - \mu)]D_1$  and  $\Delta^* = \epsilon D_1/4A$  for  $\epsilon > 0$ . Similarly, in the vicinity of either fixed point the linearized renormalization group equations  $dD_2/d\ell = -(2 - \mu)\delta D_2 + A((2d - \mu - a)/D_1)\delta\Delta$  and  $d\delta\Delta/d\ell = -|\epsilon|\delta\Delta$  with solutions of the same form as in Eqs. (4.15-4.16), i.e.,

$$\delta D_2(\ell) = \left[ \delta D_2^0 - A \frac{3\mu - 2d - 2}{2 - \mu} \frac{\delta\Delta^0}{D_1} \right] e^{-(2-\mu)\ell} - A \frac{3\mu - 2d - 2}{2 - \mu} \frac{\delta\Delta^0}{D_1} e^{-|\epsilon|\ell} \quad (4.32)$$

$$\delta\Delta(\ell) = \delta\Delta^0 e^{-|\epsilon|\ell}. \quad (4.33)$$

For the distribution function  $P(\mathbf{k}, \omega, D_1, D_2, \Delta)$  and diffusion coefficient  $D_2(\mathbf{k}, \omega, D_1, D_2, \Delta)$  we obtain again for large  $\ell$  and choosing  $\mathbf{k}e^\ell \simeq 1$  the scaling forms Eqs. (6.67) and (6.68). We also obtain the scaling form in Eq. (4.13) for  $P$ , implying that the dynamic exponent  $z$  locks onto  $\mu$ .

As in the short range case the main conclusion is that in the case of Lévy flights in a weak isotropic long range force field, the long time scaling behavior is entirely controlled by the leading anomalous Lévy term  $D_1 k^\mu$ . The random force field does not influence the Lévy flights. The long range superdiffusive behavior enables the walker to escape the inhomogeneous pinning environment and the long time behavior is the same as in the pure case.

For  $\epsilon < 0$ , i.e.,  $d > a > a_{c1}$ , we have the Gaussian fixed point  $(D_2^*, \Delta^*) = (0, 0)$  and we obtain in particular the complex scaling function in Eq. (4.14) for  $P(\mathbf{k}, \omega)$ . Implementing the matching procedure as in the short range case, we obtain to lowest order in  $\Delta$  Eqs. (4.18) and (4.24) For  $\epsilon < 0$  or  $d > a > a_{c1}$   $\Delta^* = 0$  and we have

$$D_2(\mathbf{0}, \omega, D_2, \Delta) \propto \delta \Delta^0 \omega^{(a-a_{c2})/a_{c2}} \quad (4.34)$$

$$D_2(\mathbf{k}, 0, D_2, \Delta) \propto \delta \Delta_0 k^{a-a_{c2}}, \quad (4.35)$$

where  $a_{c2} = d_{c2} = \mu$  is the second critical fall-off exponent. In the low frequency limit  $\omega \rightarrow 0$  or long wavelength limit  $\mathbf{k} \rightarrow 0$   $D_2$  vanishes for  $a > a_{c2}$  and diverges for  $a < a_{c2}$ . This behavior is in accordance with the naive perturbation theory discussed in Sec. III and in Appendix B; introducing a force correlation  $\Delta \sim p^{a-d}$  in the integrand in Eq. (3.8) for the correction  $\delta D_2$  we obtain a convergent contribution for  $a > a_{c2}$  and a diverging  $\delta D_2$  for  $a < a_{c2}$ .

For  $\epsilon > 0$  or  $a < a_{c1}$   $\Delta^* \neq 0$  and we obtain Eqs. (4.21) and (4.26) diverging in the low frequency and long wavelength limits, respectively.

Finally, we obtain for the temporal and spatial behavior of  $D_2$  for  $\epsilon < 0$

$$D_2(\mathbf{0}, t, D_2, \Delta) \propto t^{-a/a_{c2}} \quad (4.36)$$

$$D_2(\mathbf{r}, 0, D_2, \Delta) \propto r^{a_{c2}-a-d} \quad (4.37)$$

and for  $\epsilon > 0$  Eqs. (4.23) and (4.28).

The scaling properties in the isotropic long range case as compared to the short range case are conveniently summarized in Fig. 13 and Fig. 14. In Fig. 13 we have plotted the fall-off exponent as a function of  $\mu$ . The lines  $a = a_{c2}$  and  $a = a_{c1}$  delimit three regions I, II, and III. In I the diffusion coefficient  $D_2$  vanishes and the disorder is *irrelevant*, in II the diffusion coefficient  $D_2$  diverges and the disorder is *irrelevant*, and in III  $D_2$  diverges and disorder becomes *relevant*. We note that Fig. 13 is identical to Fig. 11 with the dimension  $d$  replaced by the exponent  $a$ . In Fig. 14 we have in a plot of the exponent  $a$  versus the dimension  $d$  contrasted the long range case to the short range case. The short and long range cases are delimited by the line  $d = a$ . For  $a > d$  we have the short range case, for  $a < d$  the long range case (see Sec. III). In region I delimited by  $a = a_{c1}$  and  $d = d_{c1}$   $D_2$  diverges and the disorder is *relevant*, in region II delimited by  $a = a_{c2}$  and  $d = d_{c2}$   $D_2$  diverges and the disorder is *irrelevant*, and in region I  $D_2$  vanishes and disorder is *irrelevant*. In the Brownian case  $\mu = 2$  and region II vanishes; the divergence of  $D_2$  coincides with the disorder becoming relevant for  $d = 2$  in the short range case and  $a = 2$  in the long range case, see ([27]). In Appendix B we briefly summarize the relevant aspects of the renormalization group flow in the  $\Delta - D_2$  plane.

In the case of a general anisotropic force field the fixed point structure becomes more complicated and we encounter the same features as in the Brownian case, refs. [4] and [27]. The analysis nevertheless proceeds as in the isotropic case and we therefore defer the discussion to Appendix G (the short range case) and Appendix H (the long range case).

## V. SUMMARY AND CONCLUSION

In the present paper we have discussed Lévy flights in  $d$  dimensions in a variety of quenched force fields with fall-off exponent  $a$ . The main conclusion of the paper is that the long range characteristics of the random motion, characterized by the dynamic exponent  $z$ , is essentially not influenced by the quenched force field and the exponent  $z$  locks onto the step index  $\mu$  in all cases. In other words, the long range character of the Lévy steps enables the walker to escape the inhomogeneous pinning environment created by the quenched force field.

This behavior is entirely different from the case of ordinary Brownian motion where the dynamic exponent  $z$  is enhanced, corresponding to subdiffusive behavior for  $d < 2$  in the case of short range forces and for  $a < 2$  in the case of long range forces.

Although the dynamic exponent  $z$  is unaffected by the quenched environment the phenomenon is still characterized by a critical dimension  $d_{c1}$  in the short range case and a critical fall-off exponent  $a_c$  in the long range case. The critical parameters delimit the relevance of the quenched force field. For  $d > d_{c1} = 2\mu - 2$  in the short range case and  $a > d_{c1} = 2\mu - 2$  in the long range case, the force correlations scale to zero, indicating that the quenched background

does not influence the long range walk characteristics. We note that in the Brownian case  $\mu = 2$  and, consequently,  $d_{c1} = 2$  in the short range case, coinciding with the dimension where Brownian walk becomes transparent, i.e., with a finite probability of revisiting a site and thus becoming sensitive to the force correlations.

For  $d < d_{c1}$  or  $a < a_c$  the strength of the force correlations characterized by  $\Delta$  scales to a finite (fixed point) value, showing the relevance of the quenched background. In the Brownian case this gives rise to a change of the dynamic exponent  $z$ , unlike the Lévy case where  $z$  remains unchanged

A further aspect of the Lévy case is the appearance of a second critical parameter:  $d_{c1} = \mu$  in the short range case and  $a_c = \mu$  in the long range case. These parameters delimit the behavior of the subleading diffusive term characterized by the ordinary diffusion coefficient  $D_2$ , which, of course, in the Brownian case is the leading term. For  $d > d_{c1}$  or  $a > a_c$  the wave number dependent diffusion coefficient  $D_2(\mathbf{k})$  vanishes in the long wavelength limit  $\mathbf{k} \rightarrow 0$ ; for  $d < d_{c1}$  or  $a < a_c$ , correspondingly,  $D_2(\mathbf{k})$  diverges for  $\mathbf{k} \rightarrow 0$ . In the Lévy case this behavior is subleading and does not affect the leading term characterized by the (unchanged) dynamic exponent  $z$ . The above behavior is illustrated in Figs. 11,13, and 14.

In the anisotropic short range and long range cases we encounter as in the Brownian case a more complicated fixed point and renormalization group flow structure, depicted in Figs 16 and 17. However, as mentioned above the exponent  $z$  remains locked onto  $\mu$  and we find that the behavior of the subleading diffusion coefficient  $D_2$  is the same as in the isotropic case.

Below in Table 1 we have summarized the behavior of  $D_2$  in the various cases.

	$D_2(\mathbf{k})$	$D_2(\mathbf{r})$	$D_2(\omega)$	$D_2(t)$
$d > 2\mu - 2$	$k^{d-\mu}$	$r^{\mu-2d}$	$\omega^{(d-\mu)/\mu}$	$t^{-d/\mu}$
$d < 2\mu - 2$	$k^{\mu-2}$	$r^{2-d-\mu}$	$\omega^{(\mu-2)/\mu}$	$t^{-(2\mu-2)/\mu}$
$a > 2\mu - 2$	$k^{a-\mu}$	$r^{\mu-d-a}$	$\omega^{(a-\mu)/\mu}$	$t^{-a/\mu}$
$a < 2\mu - 2$	$k^{\mu-2}$	$r^{2-d-\mu}$	$\omega^{(\mu-2)/\mu}$	$t^{-(2\mu-2)/\mu}$

TABLE I. Table of the behavior of the wave number, space, frequency and time dependent subleading ordinary diffusion coefficient in the case of short range and long range force correlations in the quenched background.



## ACKNOWLEDGMENTS

The author wishes to thank K.B. Lauritsen, L. Mikheev, M.H. Jensen, H.J. Jensen, A. Svane and T. Bohr for useful conversations.

## VI. APPENDIX

In the ensuing appendices we include more technical aspects of our calculations. In Appendix A we discuss the derivation of a Fokker-Planck equation for Lévy flights, in Appendix B we derive self energy, vertex, and force corrections to first loop order, and in Appendix C we derive renormalization group equations in the case of Lévy flights in a quenched force field. In Appendix D we consider the renormalization group flow in the isotropic short and long range cases. Appendix E we show that the dynamical exponent does not depend on whether we keep the Lévy coefficient or diffusion coefficient fixed under scaling. In Appendix F we summarize the isotropic long range case for Brownian walks. Finally Appendix G and H are devoted to a discussion of the anisotropic short and long range cases, respectively.

### A. The Fokker-Planck equation for Lévy flights

The usual derivation of the Fokker-Planck equation [45,54] depends in an essential way on the existence of the moments of the distribution. Precisely this assumption breaks down for Lévy flights for a step size distribution with  $f < 2$  and we must reconsider the derivation of the associated Fokker-Planck equation. In Sec. II we gave a heuristic derivation of the Fokker-Planck equation based on the motion in the absence of a force field. Here we derive the Fokker-Planck equation generalizing the standard procedure and relaxing the assumption of finite moments. Adapting the discussion in ref. [54] we define the functional

$$I = \int R(\mathbf{r}_2) \frac{\partial P(\mathbf{r}_2|\mathbf{r}_1, t)}{\partial t} d^d r_2, \quad (6.1)$$

where  $P(\mathbf{r}_2|\mathbf{r}_1, t)$  is the conditional probability distribution and  $R(\mathbf{r})$  is a generator function. Using the “chain rule” for a Markovian stochastic process,

$$P(\mathbf{r}_2|\mathbf{r}_1, t) = \int P(\mathbf{r}_2|\mathbf{r}, t_1) P(\mathbf{r}|\mathbf{r}_1, t - t_1) d^d r \quad (6.2)$$

and expanding in Fourier modes,  $R(\mathbf{r}) = \sum_{\mathbf{k}} e^{i\mathbf{k}\cdot\mathbf{r}} R_{\mathbf{k}}$ , we obtain, replacing  $\partial P/\partial t$  by  $(P(t + \Delta t) - P(t))/\Delta t$ ,

$$I = \sum_{\mathbf{k}} \int d^d r_2 e^{i\mathbf{k}\cdot\mathbf{r}_2} R_{\mathbf{k}} \frac{\partial P(\mathbf{r}_2|\mathbf{r}_1, t)}{\partial t} = \sum_{\mathbf{k}} \int d^d r e^{i\mathbf{k}\cdot\mathbf{r}} R_{\mathbf{k}} \left[ \int d^d r_2 \frac{e^{i\mathbf{k}\cdot(\mathbf{r}_2 - \mathbf{r})} - 1}{\Delta t} P(\mathbf{r}_2|\mathbf{r}, \Delta t) \right] P(\mathbf{r}|\mathbf{r}_1, t). \quad (6.3)$$

In order to evaluate

$$\int d^d r_2 \frac{e^{i\mathbf{k}\cdot(\mathbf{r}_2 - \mathbf{r})} - 1}{\Delta t} P(\mathbf{r}_2|\mathbf{r}, \Delta t) = \left\langle \frac{e^{i\mathbf{k}\cdot(\mathbf{r}(\Delta t) - \mathbf{r}(0))} - 1}{\Delta t} \right\rangle \quad (6.4)$$

we invoke the Langevin equation for Lévy flights (2.11),  $d\mathbf{r}/dt = \mathbf{F}(\mathbf{r}) + \boldsymbol{\eta}$  with incremental solution

$$\mathbf{r}(\Delta t) - \mathbf{r}(0) = \mathbf{F}(\mathbf{r})\Delta t + \boldsymbol{\eta}\Delta t. \quad (6.5)$$

Inserting Eq. (6.5) in Eq.(6.4), expanding and using the result  $\langle e^{i\mathbf{k}\cdot\boldsymbol{\eta}\Delta t} - 1 \rangle = -\text{const.} k^\mu \Delta t$  for a Lévy distribution (cf. Eqs. (2.3-2.4)) we obtain  $\langle (e^{i\mathbf{k}\cdot(\mathbf{F}(\mathbf{r})\Delta t + \boldsymbol{\eta}\Delta t)} - 1)/\Delta t \rangle \simeq -\text{const.} k^\mu + i\mathbf{k} \cdot \mathbf{F}(\mathbf{r})$  which, inserted in in Eq. (6.3) and requiring it to hold for any variation of  $R$ , yields the Fokker-Planck equation for Lévy flights (in momentum space),

$$\frac{\partial P(\mathbf{k}, t)}{\partial t} = -\text{const.} k^\mu P(\mathbf{k}, t) - i\mathbf{k} \cdot \sum_{\mathbf{p}} \mathbf{F}(\mathbf{k} - \mathbf{p}) P(\mathbf{p}, t) \quad (6.6)$$

## B. Self energy, vertex, and force corrections to first loop order

Here we evaluate the self energy, vertex and force corrections to lowest order for Lévy flights in a general anisotropic force field using the diagrammatic rules and diagrams in Sec. III.

The self energy correction is given by the diagrams in Fig. 7.  $\Sigma(\mathbf{k}, \omega)$  splits up in longitudinal and transverse contributions, i.e.,  $\Sigma(\mathbf{k}, \omega) = \Sigma_L(\mathbf{k}, \omega) + \Sigma_T(\mathbf{k}, \omega)$ . For  $\Sigma_L$  we have

$$\Sigma_L(\mathbf{k}, \omega) = -\lambda_L^2 \int \frac{d^d p}{(2\pi)^d} \Delta^L(\mathbf{k}/2 - \mathbf{p}) \frac{\mathbf{k} \cdot (\mathbf{k}/2 - \mathbf{p}) (\mathbf{k}/2 - \mathbf{p}) \cdot (\mathbf{k}/2 + \mathbf{p})}{(\mathbf{k}/2 - \mathbf{p})^2} G_0(\mathbf{k}/2 + \mathbf{p}, \omega). \quad (6.7)$$

In order to extract the leading contribution to  $O(k^2)$  we first symmetrize Eq. (6.7) by replacing  $\mathbf{p}$  by  $-\mathbf{p}$  and, furthermore, expanding  $G_0^{-1}(\mathbf{k}/2 \pm \mathbf{p}, \omega)$  and  $\Delta^L(\mathbf{k}/2 \pm \mathbf{p})$  for small  $k$ ,  $G_0^{-1}(\mathbf{k}/2 \pm \mathbf{p}, \omega) = G_0^{-1}(\mathbf{p}, \omega) \pm (\mathbf{p} \cdot \mathbf{k}/2)(\mu D_1 p^{\mu-2} + 2D_2)$  and  $\Delta^L(\mathbf{k}/2 \pm \mathbf{p}) = \Delta^L(\mathbf{p}) \pm (\mathbf{p} \cdot \mathbf{k}/2)(a_L - d)p^{a_L-d-2}$  we obtain to  $O(k^2)$

$$\Sigma_L(\mathbf{k}, \omega) = \frac{1}{2} k^2 \frac{\lambda_L^2}{d} \int \frac{d^d p}{(2\pi)^d} \left\{ [(d-2)G_0^{-1}(\mathbf{p}, \omega) + (\mu D_1 p^\mu + 2D_2 p^2)] \Delta^L(\mathbf{p}) + G_0^{-1}(\mathbf{p}, \omega) \Delta_2^L(a_L - d) p^{a_L-d} \right\} G_0(\mathbf{p}, \omega)^2. \quad (6.8)$$

Similarly, we find for  $\Sigma_T(\mathbf{k}, \omega)$  to  $O(k^2)$ ,

$$\Sigma_T(\mathbf{k}, \omega) = -\frac{1}{2} k^2 \frac{\lambda_T^2}{d} \int \frac{d^d p}{(2\pi)^d} (2d-2) \Delta^T(\mathbf{p}) G_0(\mathbf{p}, \omega). \quad (6.9)$$

In the static limit  $\omega \rightarrow 0$  and in the isotropic short range case,  $\lambda_L = \lambda_T = \lambda$ , and  $\Delta^{L,T}(\mathbf{p}) = \Delta$ , we obtain in particular the expression yielding Eq. (3.8),

$$\Sigma(\mathbf{k}, 0) = -\frac{1}{2} k^2 \frac{\lambda^2}{d} \Delta \int \frac{d^d p}{(2\pi)^d} \frac{D_1(d-\mu)p^\mu + D_2(d-2)p^2}{[D_1 p^\mu + D_2 p^2]^2}. \quad (6.10)$$

In the context of the momentum shell integration method discussed in Sec. III the dilution of degrees of freedom requires that the internal momenta  $\mathbf{k}/2 + \mathbf{p}$  and  $\mathbf{k}/2 - \mathbf{p}$  of the propagator and force contraction, respectively, must lie in the momentum shells  $e^{-\ell} < |\mathbf{k}/2 + \mathbf{p}| < 1$  and  $e^{-\ell} < |\mathbf{k}/2 - \mathbf{p}| < 1$ . We notice that this assignment is invariant under the symmetrization  $\mathbf{p} \rightarrow -\mathbf{p}$  performed in order to extract the leading  $k^2$  correction to  $\Sigma$ . On the shell we thus obtain for  $\Sigma(\mathbf{k}, 0)$  in Eq. (6.10) for small  $\ell$ ,

$$\Sigma(\mathbf{k}, 0) = -\frac{1}{2} k^2 \lambda^2 \Delta \frac{S_d}{(2\pi)^d} \frac{1}{d} \frac{D_1(d-\mu) + D_2(d-2)}{[D_1 + D_2]^2} \ell, \quad (6.11)$$

where  $S_d = 2\pi^{d/2}/(d/2 - 1)!$  (cf. Eq. (2.1)), leading to Eq. (3.32) for the correction  $\delta D_2$  to the diffusion coefficient.

In a completely similar manner we obtain in the general case on the shell  $p = 1$ ,

$$\Sigma(\mathbf{k}, 0) = \frac{1}{2} k^2 \frac{S_d}{(2\pi)^d} \frac{1}{d} \frac{\lambda_L^2 [(d+\mu)D_1(\Delta_1^L + \Delta_2^L) + (a_L - d)(D_1 + D_2)\Delta_2^L] - \lambda_T^2 (2d-2)(D_1 + D_2)(\Delta_1^T + \Delta_2^T)}{[D_1 + D_2]^2} \ell. \quad (6.12)$$

The vertex corrections are given by the diagrams in Fig. 8. In the isotropic short range case the correction is given in Eq. (3.9) and  $\delta\lambda$  in Eq. (3.10) follows directly, i.e., no symmetrization is required here since the correction in Eq. (3.9) is already of order  $k$ . Focusing on the corrections to  $\lambda_L$  and  $\lambda_T$  the calculation is also quite simple in the general case. We obtain

$$\delta\lambda_T = -\lambda_T \lambda_L^2 \frac{1}{d} \int \frac{d^d p}{(2\pi)^d} \Delta^L(\mathbf{p}) G_0(\mathbf{p}, 0)^2 \quad (6.13)$$

$$\delta\lambda_L = -\lambda_L^3 \frac{1}{d} \int \frac{d^d p}{(2\pi)^d} \Delta^L(\mathbf{p}) G_0(\mathbf{p}, 0) \quad (6.14)$$

and on the shell  $e^{-\ell} < p < 1$

$$\delta\lambda_T = -\lambda_T\lambda_L^2 \frac{S_d}{(2\pi)^d} \frac{1}{d} \frac{\Delta_1^L + \Delta_2^L}{[D_1 + D_2]^2} \ell \quad (6.15)$$

$$\delta\lambda_L = -\lambda_L^3 \frac{S_d}{(2\pi)^d} \frac{1}{d} \frac{\Delta_1^L + \Delta_2^L}{[D_1 + D_2]^2} \ell. \quad (6.16)$$

The force corrections are given by the diagrams in Fig. 9. In the isotropic short range case the results are given in Eqs. (3.11-3.12). In the general case we obtain the correction to the vertex function  $\Gamma(\mathbf{k}, \mathbf{p}, \mathbf{l}, \omega)$  defined diagrammatically in Fig. 6, introducing the tensors (dyadics)  $\tilde{\Delta}^L(\mathbf{k}) = [k^\alpha k^\beta / k^2] \Delta^L(\mathbf{k})$  and  $\tilde{\Delta}^T(\mathbf{k}) = [\delta^{\alpha\beta} - k^\alpha k^\beta / k^2] \Delta^T(\mathbf{k})$ ,

$$\begin{aligned} \Gamma(\mathbf{k}, \mathbf{p}, \mathbf{l}, \omega) = & -\lambda_L^2 \mathbf{k} \cdot \tilde{\Delta}^L(\mathbf{l}) \cdot \mathbf{p} - \lambda_T^2 \mathbf{k} \cdot \tilde{\Delta}^T(\mathbf{l}) \cdot \mathbf{p} \\ & + \lambda_L^4 \int \frac{d^d n}{(2\pi)^d} \mathbf{k} \cdot \tilde{\Delta}^L(\mathbf{n}) \cdot (\mathbf{p} + \mathbf{l} - \mathbf{n})(\mathbf{k} - \mathbf{n}) \cdot \tilde{\Delta}^L(\mathbf{l} - \mathbf{n}) \cdot \mathbf{p} G_0(\mathbf{k} - \mathbf{n}, \omega) G_0(\mathbf{p} + \mathbf{l} - \mathbf{n}, \omega) \\ & + \lambda_T^4 \int \frac{d^d n}{(2\pi)^d} \mathbf{k} \cdot \tilde{\Delta}^T(\mathbf{n}) \cdot (\mathbf{p} + \mathbf{l} - \mathbf{n})(\mathbf{k} - \mathbf{n}) \cdot \tilde{\Delta}^T(\mathbf{l} - \mathbf{n}) \cdot \mathbf{p} G_0(\mathbf{k} - \mathbf{n}, \omega) G_0(\mathbf{p} + \mathbf{l} - \mathbf{n}, \omega) \\ & + \lambda_L^2 \lambda_T^2 \int \frac{d^d n}{(2\pi)^d} \mathbf{k} \cdot \tilde{\Delta}^L(\mathbf{n}) \cdot (\mathbf{p} + \mathbf{l} - \mathbf{n})(\mathbf{k} - \mathbf{n}) \cdot \tilde{\Delta}^T(\mathbf{l} - \mathbf{n}) \cdot \mathbf{p} G_0(\mathbf{k} - \mathbf{n}, \omega) G_0(\mathbf{p} + \mathbf{l} - \mathbf{n}, \omega) \\ & + \lambda_T^2 \lambda_L^2 \int \frac{d^d n}{(2\pi)^d} \mathbf{k} \cdot \tilde{\Delta}^T(\mathbf{n}) \cdot (\mathbf{p} + \mathbf{l} - \mathbf{n})(\mathbf{k} - \mathbf{n}) \cdot \tilde{\Delta}^L(\mathbf{l} - \mathbf{n}) \cdot \mathbf{p} G_0(\mathbf{k} - \mathbf{n}, \omega) G_0(\mathbf{p} + \mathbf{l} - \mathbf{n}, \omega) \\ & + \lambda_L^4 \int \frac{d^d n}{(2\pi)^d} \mathbf{k} \cdot \tilde{\Delta}^L(\mathbf{n}) \cdot \mathbf{p}(\mathbf{k} - \mathbf{n}) \cdot \tilde{\Delta}^L(\mathbf{l} - \mathbf{n}) \cdot (\mathbf{p} + \mathbf{n}) G_0(\mathbf{k} - \mathbf{n}, \omega) G_0(\mathbf{p} + \mathbf{n}, \omega) \\ & + \lambda_T^4 \int \frac{d^d n}{(2\pi)^d} \mathbf{k} \cdot \tilde{\Delta}^T(\mathbf{n}) \cdot \mathbf{p}(\mathbf{k} - \mathbf{n}) \cdot \tilde{\Delta}^T(\mathbf{l} - \mathbf{n}) \cdot (\mathbf{p} + \mathbf{n}) G_0(\mathbf{k} - \mathbf{n}, \omega) G_0(\mathbf{p} + \mathbf{n}, \omega) \\ & + \lambda_L^2 \lambda_T^2 \int \frac{d^d n}{(2\pi)^d} \mathbf{k} \cdot \tilde{\Delta}^L(\mathbf{n}) \cdot \mathbf{p}(\mathbf{k} - \mathbf{n}) \cdot \tilde{\Delta}^T(\mathbf{l} - \mathbf{n}) \cdot (\mathbf{p} + \mathbf{n}) G_0(\mathbf{k} - \mathbf{n}, \omega) G_0(\mathbf{p} + \mathbf{n}, \omega) \\ & + \lambda_T^2 \lambda_L^2 \int \frac{d^d n}{(2\pi)^d} \mathbf{k} \cdot \tilde{\Delta}^T(\mathbf{n}) \cdot \mathbf{p}(\mathbf{k} - \mathbf{n}) \cdot \tilde{\Delta}^L(\mathbf{l} - \mathbf{n}) \cdot (\mathbf{p} + \mathbf{n}) G_0(\mathbf{k} - \mathbf{n}, \omega) G_0(\mathbf{p} + \mathbf{n}, \omega). \end{aligned} \quad (6.17)$$

In order to identify for example the correction to  $\Delta_1^T$  we choose  $\mathbf{k} \cdot \mathbf{l} = 0$  and take the  $\mathbf{l} \rightarrow 0$  limit. Using that  $\mathbf{k} \cdot \tilde{\Delta}^L(\mathbf{l}) \cdot \mathbf{p} = 0$ ,  $\mathbf{k} \cdot \tilde{\Delta}^T(\mathbf{l}) \cdot \mathbf{p} = \mathbf{k} \cdot \mathbf{p} \Delta^T(\mathbf{l})$ ,  $\mathbf{k} \cdot \tilde{\Delta}^T(\mathbf{n}) \cdot \mathbf{n} = 0$ , and  $\mathbf{k} \cdot \tilde{\Delta}^L(\mathbf{n}) \cdot \mathbf{n} = \mathbf{k} \cdot \mathbf{n} \Delta^L(\mathbf{n})$ , the expression (6.17) reduces considerably and we find the correction

$$\delta\Delta_1^T = \lambda_L^2 \left(1 - \frac{1}{d}\right) \int \frac{d^d p}{(2\pi)^d} \Delta^T(\mathbf{p}) \Delta^L(\mathbf{p}) G_0^2(\mathbf{p}, 0) \quad (6.18)$$

and on the shell  $e^{-\ell} < p < 1$ ,

$$\delta\Delta_1^T = \lambda_L^2 \frac{S_d}{(2\pi)^d} \left(1 - \frac{1}{d}\right) \frac{(\Delta_1^T + \Delta_2^T)(\Delta_1^L + \Delta_2^L)}{[D_1 + D_2]^2} \ell. \quad (6.19)$$

Similarly, we find the correction to  $\Delta^L$  by choosing  $\mathbf{k} = \mathbf{l}$ ,

$$\delta\Delta_1^L = \delta\Delta_1^T, \quad (6.20)$$

i.e., the force corrections in the longitudinal and transverse cases are identical.

### C. Renormalization group equations in the case of a general force field

Here we derive the renormalization group equations for a general force field to first loop order following the procedure in Sec. III. Including the corrections to  $D_2$ ,  $\lambda_L$ ,  $\lambda_T$ ,  $\Delta^L$  and  $\Delta^T$  we obtain the renormalized Fokker-Planck equation and force correlations (cf. Eqs. (3.18-3.19)),

$$(-i\omega + D_1 k^\mu + (D_2 + \delta D_2)k^2)P(\mathbf{k}, \omega) = P_0(\mathbf{k}) + (\lambda_L + \delta\lambda_L) \int \frac{d^d p}{(2\pi)^d} (-i)\mathbf{k} \cdot \mathbf{E}(\mathbf{k} - \mathbf{p})P(\mathbf{p}, \omega) \\ + (\lambda_T + \delta\lambda_T) \int \frac{d^d p}{(2\pi)^d} (-i)\mathbf{k} \cdot \mathbf{B}(\mathbf{k} - \mathbf{p})P(\mathbf{p}, \omega) \quad (6.21)$$

$$\langle E^\alpha(\mathbf{k})E^\beta(\mathbf{p}) \rangle_F = (\Delta^L(\mathbf{k}) + \delta\Delta^L(\mathbf{k})) \left[ \frac{k^\alpha k^\beta}{k^2} \right] (2\pi)^d \delta(\mathbf{k} + \mathbf{p}) \quad (6.22)$$

$$\langle B^\alpha(\mathbf{k})B^\beta(\mathbf{p}) \rangle_F = (\Delta^T(\mathbf{k}) + \delta\Delta^T(\mathbf{k})) \left[ \delta^{\alpha\beta} - \frac{k^\alpha k^\beta}{k^2} \right] (2\pi)^d \delta(\mathbf{k} + \mathbf{p}), \quad (6.23)$$

where  $\mathbf{k}$  and  $\mathbf{p}$  after the momentum shell integration now range in the interval  $1 < k, p < e^{-\ell}$ . Renormalizing wave numbers, frequency, and distribution as in Eqs(3.20-3.22) and  $\mathbf{E}$  and  $\mathbf{B}$  according to  $\mathbf{E}'(\mathbf{k}') = \exp(-\beta_L(\ell))\mathbf{E}(\mathbf{k})$ , and  $\mathbf{B}(\mathbf{k}') = \exp(-\beta_T(\ell))\mathbf{B}(\mathbf{k})$ , where  $\alpha$  and  $\beta_{L,T}$  are given by Eqs. (3.30-3.31) with  $u$  replaced by  $u_{L,T}$  we obtain a renormalized Fokker-Planck equation and force correlations of the same form as in Eqs. (3.24-3.25). Furthermore, from the expressions in Eqs. (2.23-2.24) for  $\Delta^T(\mathbf{k})$  and  $\Delta^L(\mathbf{k})$  we identify scale dependent parameters and obtain the renormalization group equations

$$D'_1(\ell) = D_1 e^{-\mu\ell + \alpha} \quad (6.24)$$

$$D'_2(\ell) = (D_2 + \delta D_2) e^{-2\ell} \quad (6.25)$$

$$\lambda'_L(\ell) = (\lambda_L + \delta\lambda_L) e^{-(1+d)\ell + \alpha + \beta_L} \quad (6.26)$$

$$\lambda'_T(\ell) = (\lambda_T + \delta\lambda_T) e^{-(1+d)\ell + \alpha + \beta_T} \quad (6.27)$$

$$\Delta_1^{L'}(\ell) = (\Delta_1^L + \delta\Delta_1^L) e^{d\ell - 2\beta_L} \quad (6.28)$$

$$\Delta_2^{L'}(\ell) = \Delta_2^L e^{d\ell - 2\beta_L - \ell(\alpha_L - d)} \quad (6.29)$$

$$\Delta_1^{T'}(\ell) = (\Delta_1^T + \delta\Delta_1^T) e^{d\ell - 2\beta_T} \quad (6.30)$$

$$\Delta_2^{T'}(\ell) = \Delta_2^T e^{d\ell - 2\beta_T - \ell(\alpha_T - d)} \quad (6.31)$$

or in differential form the Eqs. (3.42-3.47). We have here again fixed the vertex constants to  $\lambda_{L,T} = 1$  by choosing  $u_L = 1 + d - z - \lambda_L^{-1} \delta\lambda_L/\ell$  and  $u_T = 1 + d - z - \lambda_T^{-1} \delta\lambda_T/\ell$ .

## D. The renormalization group flow in the isotropic case

### 1. The isotropic short range case

Eliminating  $\ell$  in Eqs. (4.15) and (4.16) and setting  $\mu = d_{c_2}$  and  $\epsilon = d_{c_1} - d$  we obtain

$$\delta D_2 = \left[ \delta D_2^0 + A \frac{\delta\Delta^0}{D_1} \right] \left[ \frac{\delta\Delta}{\delta\Delta^0} \right]^{(2-d_{c_2})/|d_{c_1}-d|} - \frac{A}{D_1} \delta\Delta. \quad (6.32)$$

In Fig. 15 we have depicted the renormalization group flow about the Gaussian fixed point  $(\Delta^*, D_2^*) = (0, 0)$  in the three cases: a)  $d > d_{c_2}$ , b)  $d = d_{c_2}$ , and c)  $d_{c_2} > d > d_{c_1}$ . In the case a) for  $d > d_{c_2}$ , corresponding to region I in Fig. 11, the first term in Eq. (6.32) dominates and near the fixed point  $\delta D_2 \sim [\delta D_2^0 + A\delta\Delta^0/D_1][\delta\Delta/\delta\Delta^0]^{(2-d_{c_2})/|d_{c_1}-d|}$ , i.e., the trajectories approach the fixed point with vertical slope except for the trajectories originating from the domain of initial values on the line  $\delta D_2^0 = -(A/D_1)\delta\Delta^0$ , corresponding to the position of the non-trivial fixed point emerging below  $d_{c_1}$ . In this regime  $D_2$  vanishes as discussed above. In the case b) for  $d = d_{c_2}$ , the marginal case, we have  $\delta D_2 = (\delta D_2^0/\delta\Delta^0)\delta\Delta$  and the trajectories approach the fixed point with constant slope, i.e., the linear scaling regime depends on  $\mu$  and becomes largest for  $\mu = d$ , precisely the case where naive perturbation theory or the scaling analysis above yield a divergent  $D_2$ . In the case c) for  $d_{c_1} < d < d_{c_2}$ , corresponding to region II in Fig. 11, we have  $\delta D_2 = -(A/D_1)\delta\Delta$ . The trajectories now approach the fixed point with a constant slope  $-A/D_1$ , except for trajectories with  $\delta\Delta^0 = 0$  which lie on the line  $\Delta = 0$ .

### 2. The isotropic long range case

Eliminating  $\ell$  in the renormalization group equations (4.32-4.33) we have

$$\delta D_2 = \left[ \delta D_2^0 + A \frac{3\mu - 2d - 2}{2 - \mu} \frac{\delta \Delta^0}{D_1} \right] \left[ \frac{\delta \Delta}{\delta \Delta^0} \right]^{(2-d_{c2})/|a_{c1}-a|} - A \frac{3\mu - 2d - 2}{2 - \mu} \delta \Delta. \quad (6.33)$$

Focusing on the flow about the Gaussian fixed point  $(\Delta^*, D_2^*) = (0, 0)$  the discussion in the isotropic short range case above applies with  $d$  replaced by  $a$ . For  $d > a > \mu$  the trajectories approach the fixed point with vertical slope except for the trajectories originating from the domain of initial values on the line  $\delta D_2^0 = -(A(3\mu - 2d - 2)/(2 - \mu)D_1) \delta \Delta^0$ , corresponding to the position of the non-trivial fixed point emerging below  $2\mu - 2$ . In the marginal case  $\mu = a$  the trajectories approach the fixed point with constant slope, i.e., the linear scaling regime depends on  $\mu$  and becomes largest for  $\mu = a$ , precisely the case where naive perturbation theory or the scaling analysis above yield a divergent  $D_2$ . For  $a < \mu$  the trajectories approach the fixed point with constant slope  $-A(3\mu - 2d - 2)/(2 - \mu)D_1$ , except for trajectories with  $\delta \Delta^0 = 0$  which lie on the line  $\Delta = 0$ . Fig. 15 also applies in the long range case with  $d$  replaced by  $a$  but note that the slope  $-A/D_1$  is replaced by  $-A(3\mu - 2d - 2)/(2 - \mu)D_1$ .

### E. Keeping the ordinary diffusion coefficient constant under renormalization

We here briefly repeat our renormalization group analysis but now keeping the diffusion coefficient  $D_2$  fixed under scaling. Limiting our discussion to the behavior near the Gaussian fixed point  $\Delta^* = 0$  we thus obtain from Eqs. (3.39-3.41)  $z = 2$  and the renormalization group equations  $dD_1/d\ell = (2 - \mu)D_1$  and  $d\Delta/d\ell = (2 - d)\Delta$  with solutions  $D_1 = D_1^0 \exp((2 - \mu)\ell)$  and  $\Delta = \Delta^0 \exp((2 - d)\ell)$ . From the homogeneity relation (4.9) we have, setting  $\alpha(\ell) = 2\ell$ ,  $P(\mathbf{k}, \omega, D_1, \Delta) = e^{2\ell} P(\mathbf{k}e^\ell, \omega e^{2\ell}, D_1^0 e^{(2-\mu)\ell}, \Delta^0 e^{(2-d)\ell})$ , which forms the basis for our scaling analysis. Choosing  $\mathbf{k}e^\ell \simeq 1$  we deduce the scaling form  $P(\mathbf{k}, \omega, D_1, \Delta) = k^{-2} P(1, \omega/k^2, D_1^0 k^{\mu-2}, \Delta^0 k^{d-2})$ . Note, however, that this form does not imply  $z = 2$  since  $D_1^0 k^{\mu-2}$  and  $\Delta^0 k^{d-2}$  diverge in the long wavelength limit  $k \rightarrow 0$ . In fact choosing  $k$  such that  $\Delta^0 k^{d-2} \ll 1$  we obtain perturbatively,  $P(\mathbf{k}, \omega, D_1, \Delta) = k^{-2} (-i\omega/k^2 + D_1^0 k^{\mu-2} + D_2 + \text{const.} \Delta^0 k^{d-2})^{-1}$  or  $P(\mathbf{k}, \omega, D_1, \Delta) = (-i\omega + D_1^0 k^\mu + D_2 k^2 + \text{const.} \Delta^0 k^d)^{-1}$  similar to our previous results and implying the dynamical exponent  $z = \mu$ .

### F. The isotropic long range case for Brownian walks

Here we recover the well-known results in the Brownian case to first loop order [4,27]. The renormalization group equations in the isotropic long range Brownian case are extracted from the general equations (3.42-3.47) by setting  $\mu = 2, D_1 = 0, D_2 = D, \Delta_1^{L,T} = 0, \Delta_2^{L,T} = \Delta$ , and  $a_{L,T} = a$ , i.e.,

$$\frac{dD}{d\ell} = (z - 2)D + A(2d - a - 2) \frac{\Delta}{D} \quad (6.34)$$

$$\frac{d\Delta}{d\ell} = (2z - 2 - a)\Delta - 4A \frac{\Delta^2}{D^2}. \quad (6.35)$$

Keeping  $D$  fixed we have  $z = 2 - A(2d - a - 2)\Delta/D^2$  and the equation for  $\Delta$ ,

$$\frac{d\Delta}{d\ell} = (2 - a)\Delta - 2A(2d - a) \frac{\Delta^2}{D^2}. \quad (6.36)$$

The expansion parameter is  $2 - a$ . For  $2 - a < 0$  we obtain the Gaussian fixed point  $\Delta^* = 0$ , the disorder is irrelevant and  $z$  locks onto 2, characterizing ordinary diffusion. For  $2 - a > 0$  we have the non-trivial fixed point  $\Delta^* = (2 - a)D^2/2A(2d - a)$  and the dynamic exponent

$$z = 2 - \frac{d - 2}{d - 1}(2 - a), \quad (6.37)$$

signalling anomalous diffusion [27], due to the interference of the quenched long range force correlations with the Brownian walk. In the vicinity of either fixed point we have  $\Delta(\ell) = \text{const.} \exp(-|2 - a|\ell) + \Delta^*$  and we obtain scaling relations for the distribution  $P(\mathbf{k}, \omega, \Delta)$  and the wave number and frequency dependent diffusion coefficient  $D(\mathbf{k}, \omega, \Delta)$ ,

$$P(\mathbf{k}, \omega, \Delta) = e^{z\ell} P(\mathbf{k}e^\ell, \omega e^{z\ell}, \Delta^* + \text{const.} e^{-|2-a|\ell}) \quad (6.38)$$

$$D(\mathbf{k}, \omega, \Delta) = e^{(2-z)\ell} D(\mathbf{k}e^\ell, \omega e^{z\ell}, \Delta^* + \text{const.} e^{-|2-a|\ell}). \quad (6.39)$$

Similar to our discussion in Sec. IV we infer from Eq. (6.38) the dynamic exponent  $z$  and from Eq. (6.39), choosing  $\omega e^{z\ell} \simeq 1$  and  $\mathbf{k} e^\ell \simeq 1$ ,  $D(\mathbf{0}, \omega, \Delta) \propto \omega^{-(2-z)/z} [\Delta^* + \text{const.} \omega^{-|2-a|/z}]$  and  $D(\mathbf{k}, 0, \Delta) \propto k^{-(2-z)} [\Delta^* + \text{const.} k^{|2-a|}]$ . For  $a > 2$  we have  $\Delta^* = 0$  and  $z = 2$ , i.e.,

$$D(\mathbf{0}, \omega, \Delta) \propto \omega^{(a-2)/2} \quad (6.40)$$

$$D(\mathbf{k}, 0, \Delta) \propto k^{a-2} \quad (6.41)$$

which vanish in the  $\mathbf{k} \rightarrow 0$  and  $\omega \rightarrow 0$  limits, and for the temporal and spatial behavior,

$$D(\mathbf{0}, t, \Delta) \propto t^{-a/2} \quad (6.42)$$

$$D(\mathbf{r}, 0, \Delta) \propto r^{2-a-d} . \quad (6.43)$$

For  $a < 2$  we have  $\Delta^* > 0$  and  $z$  given by Eq. (6.37) and

$$D(\mathbf{0}, \omega, \Delta) \propto \Delta^* \omega^{-\frac{1}{2}(\frac{d-2}{d-1})(2-a)} \quad (6.44)$$

$$D(\mathbf{k}, 0, \Delta) \propto \Delta^* \mathbf{k}^{-(\frac{d-2}{d-1})(2-a)} , \quad (6.45)$$

where the behavior of  $D$  depends also on the dimension of the system  $d$  [4,27]. Also,

$$D(\mathbf{0}, t, \Delta) \propto \Delta^* t^{\frac{1}{2}(\frac{d-2}{d-1})(2-a)-1} \quad (6.46)$$

$$D(\mathbf{r}, 0, \Delta) \propto \Delta^* r^{(\frac{d-2}{d-1})(2-a)-d} . \quad (6.47)$$

## G. The anisotropic short range case

Generally the quenched force field must be expected to be anisotropic consisting of a transverse divergence-free part  $\mathbf{B}$  and a longitudinal curl-free part  $\mathbf{E}$ . The vector character of  $\mathbf{F}$  is reflected in the transverse and longitudinal correlation functions  $\Delta^T$  and  $\Delta^L$ , respectively, introduced in Sec. II. The case of Brownian motion in a short range anisotropic force field has been discussed to first loop order in refs. [26,35]. As in the isotropic case treated in refs. [18,20] to second loop order, the critical dimension is  $d_{c1} = 2$ ; below  $d_{c1}$  the long time behavior is controlled by the isotropic fixed point  $\Delta_T^* = \Delta_L^* = \Delta^*$ , giving rise to anomalous subdiffusion. However, at intermediate times the diffusional character is controlled by a transverse fixed point  $\Delta_T^* \neq 0, \Delta_L^* = 0$ .

### 1. The Brownian case

In order to clearly illustrate how the Lévy case differs from the Brownian case we briefly discuss the renormalization group equations in the Brownian case. Setting  $D_1 = 0, D_2 = D, \Delta_1^{L,T} = \Delta_{L,T}$ , and  $\Delta_2^{L,T} = 0$ , we obtain from the general equations (3.42-3.47)

$$\frac{dD}{d\ell} = (z-2)D + A \frac{(2d-2)\Delta_T - d\Delta_L}{D^2} . \quad (6.48)$$

$$\frac{d\Delta_T}{d\ell} = (2z-d-2)\Delta_T - 2A(3-d) \frac{\Delta_L \Delta_T}{D^2} . \quad (6.49)$$

$$\frac{d\Delta_L}{d\ell} = (2z-d-2)\Delta_L - 4A \frac{\Delta_L^2}{D^2} + 2A(d-1) \frac{\Delta_L \Delta_T}{D^2} . \quad (6.50)$$

Keeping  $D$  fixed, we choose  $z = 2 - A(2(d-1)\Delta_T - d\Delta_L)/D^2$  and we have the equations for  $\Delta_T$  and  $\Delta_L$ ,

$$\frac{d\Delta_T}{d\ell} = (2-d)\Delta_L - 2A \frac{2(d-1)\Delta_T^2 + (3-2d)\Delta_L \Delta_T}{D^2} \quad (6.51)$$

$$\frac{d\Delta_L}{d\ell} = (2-d)\Delta_L - 2A \frac{(d-1)\Delta_L \Delta_T + (2-d)\Delta_L^2}{D^2} . \quad (6.52)$$

Above the critical dimension  $d_{c1} = 2$  we obtain the stable Gaussian fixed point  $(\Delta_L^*, \Delta_T^*) = (0, 0)$ , corresponding to normal diffusion for  $z = 2$  and irrelevance of the quenched force field. Below  $d_{c1}$  to  $O(2-d)$  we obtain the

stable isotropic fixed point  $(\Delta_L^*, \Delta_T^*) = [(2-d)D^2/2A, (2-d)D^2/2A]$ , controlling the long time anomalous behavior characterized by  $z = 2 + 2(2-d)^2$  evaluated to second loop order  $O((2-d)^2)$  [18,20] and the unstable anisotropic transverse fixed point  $(\Delta_L^*, \Delta_T^*) = (0, (2-d)D^2/4A)$ , determining the cross-over at intermediate times. We shall not pursue the Brownian case further here but refer to refs. [26,35,27,49–52].

## 2. The Lévy case

In the Lévy case we proceed as in Section IV, setting  $z = \mu$  in order to fix  $D_1, \Delta_1^{L,T} = \Delta_{L,T}$ , and  $\Delta_2^{L,T} = 0$ , the general equations (3.42)-(3.47) imply the renormalization group equations

$$\frac{dD_2}{d\ell} = (\mu - 2)D_2 + A \frac{(D_1(2 - \mu - d) - D_2d)\Delta_L + (D_1 + D_2)(2d - 2)\Delta_T}{(D_1 + D_2)^2} \quad (6.53)$$

$$\frac{d\Delta_L}{d\ell} = \epsilon\Delta_L - 2A \frac{2\Delta_L^2 - (d-1)\Delta_L\Delta_T}{[D_1 + D_2]^2} \quad (6.54)$$

$$\frac{d\Delta_T}{d\ell} = \epsilon\Delta_T - 2A(3-d) \frac{\Delta_L\Delta_T}{[D_1 + D_2]^2}, \quad (6.55)$$

where  $\epsilon = d_{c1} - d = 2\mu - 2 - d$ .

Again we observe that irrespective of the vector character of the random force  $\mathbf{F}$  the dynamic exponent  $z$  locks onto the Lévy index  $\mu$ , owing to the long range character of the Lévy steps. The equations (6.53-6.55) also have three fixed points:

$$(D_2^*, \Delta_L^*, \Delta_T^*) = (0, 0, 0) \quad (\text{Gaussian}) \quad (6.56)$$

$$(D_2^*, \Delta_L^*, \Delta_T^*) = \left( -\epsilon \frac{D_1}{2(3-d)}, \epsilon \frac{D_1^2}{2A(3-d)}, \epsilon \frac{D_1^2}{2A(3-d)} \right) \quad (\text{isotropic}) \quad (6.57)$$

$$(D_2^*, \Delta_L^*, \Delta_T^*) = \left( \frac{\epsilon}{4} \frac{D_1(4-3\mu)}{2-\mu}, \epsilon \frac{D_1^2}{4A}, 0 \right) \quad (\text{longitudinal}) \quad (6.58)$$

In order to examine the stability of the fixed points we derive renormalization group equations to  $O(\epsilon)$ . Setting  $D_2(\ell) = D_2^* + \delta D(\ell)$ ,  $\Delta_L(\ell) = \Delta_L^* + \delta \Delta_L(\ell)$ , and  $\Delta_T(\ell) = \Delta_T^* + \delta \Delta_T(\ell)$ , we have

$$\begin{aligned} \frac{d\delta D_2}{d\ell} = & \left( \mu - 2 + A \frac{(d+2\mu-4)\Delta_L^* - (2d-2)\Delta_T^*}{D_1^2} \right) \delta \Delta_2 \\ & + A \frac{D_1(2-\mu-d) + D_2^*(2\mu+d-4)}{D_1^2} \delta \Delta_L \\ & + A \frac{(2d-2)(D_1 - D_2^*)}{D_1^2} \delta \Delta_T \end{aligned} \quad (6.59)$$

$$\frac{d\delta \Delta_L}{d\ell} = \left( \epsilon - 2A \frac{4\Delta_L^* - (d-1)\Delta_T^*}{D_1^2} \right) \delta \Delta_L + \left( \frac{2A(d-1)\Delta_L^*}{D_1^2} \right) \delta \Delta_T \quad (6.60)$$

$$\frac{d\delta \Delta_T}{d\ell} = \left( \epsilon - 2A(3-d) \frac{\Delta_L^*}{D_1^2} \right) \delta \Delta_T - \left( 2A(3-d) \frac{\Delta_T^*}{D_1^2} \right) \delta \Delta_L. \quad (6.61)$$

In the vicinity of the Gaussian fixed point we have the solution

$$\begin{aligned} \delta D_2(\ell) = & \left( \delta D_2^0 + \frac{A}{D_1} \left( \frac{2-\mu-d}{d-\mu} \delta \Delta_L^0 + \frac{2(d-1)}{d-\mu} \delta \Delta_T^0 \right) \right) e^{-(2-\mu)\ell} \\ & - \frac{A}{D_1} \left( \frac{(2-\mu-d)}{d-\mu} \delta \Delta_L^0 + \frac{2(d-1)}{d-\mu} \delta \Delta_T^0 \right) e^{\epsilon\ell} \end{aligned} \quad (6.62)$$

$$\delta \Delta_L(\ell) = \delta \Delta_L^0 e^{\epsilon\ell} \quad (6.63)$$

$$\delta \Delta_R(\ell) = \delta \Delta_T^0 e^{\epsilon\ell} \quad (6.64)$$

and the fixed point is stable for  $\epsilon < 0$ , i.e.,  $d > d_{c1} = 2\mu - 2$ .

Eliminating  $\ell$  we obtain for the flow in the  $(D_2, \Delta_L, \Delta_T)$  space for  $\epsilon < 0$

$$\delta D_2 = \left[ \delta D_2^0 + \frac{A}{D_1} \left( \frac{2-\mu-d}{d-\mu} \delta \Delta_L^0 + \frac{2(d-1)}{d-\mu} \delta \Delta_T^0 \right) \right] \left[ \frac{\delta \Delta_{L,T}}{\delta \Delta_{L,T}^0} \right]^{(2-\mu)/|\epsilon|} - \frac{A}{D_1} \left[ \frac{2-\mu-d}{d-\mu} \delta \Delta_L + \frac{2(d-1)}{d-\mu} \delta \Delta_T \right] \quad (6.65)$$

and the discussion in the isotropic case applies with a few modifications. For  $d > d_{c2}$  the trajectories approach the fixed point with vertical slope with exception of trajectories lying in the plane

$$\delta D_2 = -\frac{A}{D_1} \left[ \frac{2-\mu-d}{d-\mu} \delta \Delta_L + \frac{2(d-1)}{d-\mu} \delta \Delta_T \right] . \quad (6.66)$$

In the limiting case  $d = \mu$  the trajectories approach the fixed point with constant slope, i.e., the linear scaling regime depends on  $\mu$  and becomes largest for  $\mu = d$ , corresponding to the case where naive perturbation theory yields a divergent diffusion coefficient. Finally, for  $d_{c1} < \mu < d$  the flow approaches the fixed point tangentially to the plane defined by Eq. (6.66). The characteristics of the flow are depicted in Fig. 15.

The scaling analysis of  $P$  and  $D_2$  also proceeds as in the isotropic case. Suppressing the dependence on  $D_1$  which is kept fixed we define  $P(\mathbf{k}, \omega, D_2, \Delta_L, \Delta_T) = \langle P(\mathbf{k}, \omega) \rangle_F$  and we obtain the homogeneity relations:

$$P(\mathbf{k}, \omega, D_2, \Delta_L, \Delta_T) = e^{\mu \ell} P(\mathbf{k}, e^\ell, \omega e^{\mu \ell}, D_2(\ell), \Delta_L(\ell), \Delta_T(\ell)) \quad (6.67)$$

$$D_2(\mathbf{k}, \omega, D_2, \Delta_L, \Delta_T) = e^{(2-\mu)\ell} D_2(\mathbf{k} e^\ell, \omega e^{\mu \ell}, D_2(\ell), \Delta_L(\ell), \Delta_T(\ell)) . \quad (6.68)$$

For  $\epsilon < 0$ , i.e.,  $d > d_{c1}$ , where the stable Gaussian fixed point controls the scaling behavior, we obtain, of course, the same scaling properties of  $P$  as in the isotropic case, i.e., the dynamic exponent  $z = \mu$  and  $P$  is given by the scaling functions in Eqs. (6.67) and (4.14). For the diffusion coefficient  $D_2$  we obtain, correspondingly,

$$D_2(\mathbf{k}, \omega, D_2, \Delta_L, \Delta_T) = e^{(2-\mu)\ell} D_2(\mathbf{k} e^\ell, \omega e^{\mu \ell}, \Delta_L e^{-|\epsilon|\ell}, \Delta_T e^{-|\epsilon|\ell}) \quad (6.69)$$

In the long wavelength limit  $\mathbf{k} \rightarrow 0$  and using the perturbative result  $D_2 \sim \alpha \Delta_L + \beta \Delta_T$  we have, setting  $\omega e^{\mu \ell} \sim 1$  and  $\mathbf{k} e^{\mu \ell} \sim 1$ , the same results as in the isotropic case given by Eqs. (4.19) and (4.25) and the corresponding results for the temporal and spatial behavior in Eqs. (4.22) and (4.27).

Below the critical dimension  $d_{c1}$  in the neighborhood of the isotropic fixed point in Eq. (6.57) we obtain from Eqs. (6.60) and (6.61) the solutions for  $\delta \Delta_L$  and  $\delta \Delta_T$ ,

$$\delta \Delta_L(\ell) = -\frac{(3-d)}{2(d-2)} \left( \delta \Delta_L^0 - \frac{d-1}{3-d} \delta \Delta_T^0 \right) e^{-|\epsilon|\ell} + \frac{d-1}{2(d-2)} (\delta \Delta_L^0 - \delta \Delta_T^0) e^{-|\epsilon|\frac{d-1}{3-d}\ell} \quad (6.70)$$

$$\delta \Delta_T(\ell) = -\frac{3-d}{2(d-2)} \left( \delta \Delta_L^0 - \frac{d-1}{3-d} \delta \Delta_T^0 \right) e^{-|\epsilon|\ell} + \frac{3-d}{2(d-2)} (\delta \Delta_L^0 - \delta \Delta_T^0) e^{-|\epsilon|\frac{d-1}{3-d}\ell} \quad (6.71)$$

and we conclude that the isotropic fixed point is stable for  $1 < d < d_{c1}$ .

Similarly, near the anisotropic fixed point in Eq. (6.58) we have

$$\delta \Delta_L(\ell) = \left( \delta \Delta_L^0 - \frac{d-1}{3-d} \delta \Delta_T^0 \right) e^{-|\epsilon|\ell} + \frac{d-1}{3-d} \delta \Delta_T^0 e^{-|\epsilon|\frac{1-d}{3-d}\ell} \quad (6.72)$$

$$\delta \Delta_T(\ell) = \delta \Delta_T^0 e^{-|\epsilon|\frac{1-d}{2}\ell} \quad (6.73)$$

and we infer that the anisotropic fixed point is stable for  $d < 1$ . In Fig. 16 we have depicted the renormalization group flow in the  $(\Delta_T, \Delta_L)$  plane in the three cases a)  $d > d_{c1}$ , b)  $d_{c1} > d > 1$ , and c)  $d < 1$ .

Finally, below  $d_{c1}$  we obtain for the diffusion coefficient  $D_2$  the same result as in the isotropic case in Eqs.(4.21), (4.26), (4.23) and (4.28).

## H. The anisotropic long range case

We finally discuss the anisotropic long range case. In Sec. III we have given the general renormalization group equations in the case of two separate fall-off exponents  $a_L$  and  $a_T$  for the longitudinal and transverse force correlations, respectively. For simplicity we here only consider the case of a common fall-off exponent  $a = a_T = a_L < d$ . Keeping



$D_1$  fixed by locking  $z$  onto  $\mu$  and setting  $\Delta_1^{L,T} = 0$  and  $\Delta_2^{L,T} = \Delta_{L,T}$  we extract from Eqs. (3.42)-(3.47) the renormalization group equations

$$\begin{aligned} \frac{dD_2}{d\ell} &= (\mu - 2)D_2 + A \frac{D_1(2 - \mu - a) - D_2 a}{(D_1 + D_2)^2} \Delta_L \\ &\quad + A \frac{D_1(2d - 2) + D_2(2d - 2)}{(D_1 + D_2)^2} \Delta_T \end{aligned} \quad (6.74)$$

$$\frac{d\Delta_L}{d\ell} = \epsilon \Delta_L - 4A \frac{\Delta_L^2}{(D_1 + D_2)^2} \quad (6.75)$$

$$\frac{d\Delta_T}{d\ell} = \epsilon \Delta_T - 4A \frac{\Delta_L \Delta_T}{(D_1 + D_2)^2}, \quad (6.76)$$

where we have introduced the expansion parameter  $\epsilon = 2\mu - 2 - a = d_{c1} - a$ . To first order in  $\epsilon$  we identify the usual Gaussian fixed point  $(\Delta_L^*, \Delta_T^*) = (0, 0)$  and a line of non-trivial fixed points  $\Delta_L^* = \epsilon D_1^2 / 4A$ . We note that here there is no isolated non-trivial fixed point unlike in the short range case discussed above [53].

To linear order in  $\epsilon$  we obtain in the vicinity of the respective fixed points, setting  $\Delta_{L,T} = \Delta_{L,T}^* + \delta\Delta_{L,T}$ ,

$$\frac{d\delta\Delta_L}{d\ell} = \left( \epsilon - \frac{8A}{D_1^2} \Delta_L^* \right) \delta\Delta_L \quad (6.77)$$

$$\frac{d\delta\Delta_T}{d\ell} = \left( \epsilon - \frac{4A}{D_1^2} \Delta_L^* \right) \delta\Delta_T - \frac{4A}{D_1^2} \Delta_L^* \delta\Delta_L. \quad (6.78)$$

In the neighborhood of the Gaussian fixed point we have the solutions  $\delta\Delta_T(\ell) = \delta\Delta_T^0 e^{\epsilon\ell}$  and  $\delta\Delta_L(\ell) = \delta\Delta_L^0 e^{\epsilon\ell}$ , showing that the fixed point is stable for  $\epsilon < 0$ , i.e., for  $d > a > 2\mu - 2$  (note that  $a < d$  in the long range case). Eliminating the scaling parameter  $\ell$  we obtain for the flow in the  $\Delta_L - \Delta_T$  plane  $\delta\Delta_T = (\delta\Delta_T^0 / \delta\Delta_L^0) \delta\Delta_L$ , i.e., the trajectories approach the fixed point with constant slope [53]. Similarly for the scale dependent diffusion coefficient  $D_2(\ell)$  we have

$$\delta D_2 = \left[ \delta D_2^0 + \frac{A}{D_1} \left( \frac{2 - \mu - a}{d - \mu} \delta\Delta_L^0 + \frac{d(d-1)}{a - \mu} \delta\Delta_T^0 \right) \right] e^{(2-\mu)\ell} - \frac{A}{D_1} \left[ \frac{2 - \mu - a}{a - \mu} \delta\Delta_L^0 + \frac{2(d-1)}{a - \mu} \delta\Delta_T^0 \right] e^{\epsilon\ell}. \quad (6.79)$$

Eliminating  $\ell$  we obtain for the flow for  $\epsilon < 0$

$$\begin{aligned} \delta D_2 &= \left[ \delta D_2^0 + \frac{A}{D_1} \left( \frac{2 - \mu - a}{a - \mu} \delta\Delta_L^0 + \frac{2(d-1)}{a - \mu} \delta\Delta_T^0 \right) \right] \left[ \frac{\delta\Delta_{L,T}}{\delta\Delta_{L,T}^0} \right]^{(2-\mu)/|\epsilon|} \\ &\quad - \frac{A}{D_1} \left[ \frac{2 - \mu - d}{a - \mu} \delta\Delta_L + \frac{2(d-1)}{a - \mu} \delta\Delta_T \right] \end{aligned} \quad (6.80)$$

and the discussion in the anisotropic short range case applies with  $d$  replaced by  $a$ .

The scaling analysis of  $P$  and  $D_2$  also proceeds as before. We have the general homogeneity relations in Eqs. (6.67-6.68). For  $\epsilon < 0$ , i.e.,  $a > 2\mu - 2$ , the Gaussian fixed point controls the scaling behavior. The dynamic exponent  $z = \mu$  and  $P$  is given by Eqs. (6.67) and (4.14). For  $D_2$  we obtain

$$D_2(\mathbf{k}, \omega, D_2, \Delta_L, \Delta_T) = e^{(2-\mu)\ell} D_2 \left( \mathbf{k} e^\ell, \omega e^{\mu\ell}, \Delta_L e^{-|\epsilon|\ell}, \Delta_T e^{-|\epsilon|\ell} \right) \quad (6.81)$$

and using the perturbative result  $D_2 \propto \alpha \Delta_L + \beta \Delta_T$  we find, setting  $\omega e^{\mu\ell} \simeq 1$ , and  $\mathbf{k} e^\ell \simeq 1$ , respectively,

$$D_2(\mathbf{0}, \omega, D_2, \Delta_L, \Delta_T) \propto \omega^{(a-\mu)/\mu} \quad (6.82)$$

$$D_2(\mathbf{k}, 0, D_2, \Delta_L, \Delta_T) \propto k^{a-\mu} \quad (6.83)$$

and

$$D_2(\mathbf{0}, t, D_2, \Delta_L, \Delta_T) \propto t^{-a/\mu} \quad (6.84)$$

$$D_2(\mathbf{r}, 0, D_2, \Delta_L, \Delta_T) \propto r^{\mu-d-a} \quad (6.85)$$

For  $\epsilon > 0$ , i.e.,  $a < 2\mu - 2$ , we have in the vicinity of the stable line of fixed points  $\delta\Delta_L(\ell) = \delta\Delta_L^0 e^{-\epsilon\ell}$  and  $\delta\Delta_T(\ell) = \delta\Delta_T^0 + \delta\Delta_L^0 (\Delta_T^* / \Delta_L^*) (e^{-\epsilon\ell} - 1)$  or eliminating  $\ell$   $\delta\Delta_T - \delta\Delta_T^0 = (\Delta_T^* / \Delta_L^*) (\delta\Delta_L - \delta\Delta_L^0)$ , showing that the

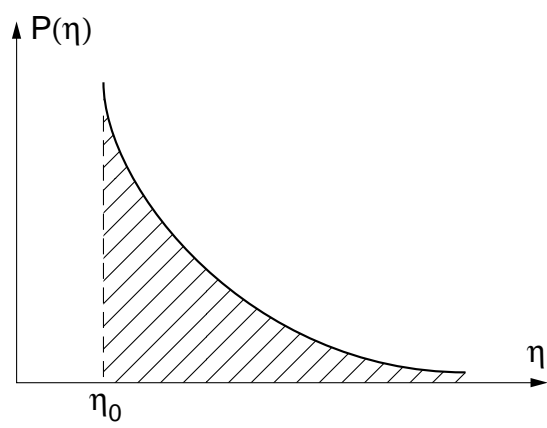
trajectories approach the line of fixed points  $\Delta_L^* = \epsilon_L D_1^2/4A$  with slope  $\Delta_T^*/\Delta_L^*$ . In Fig. 17 we have shown the renormalization group flow in the  $\Delta_T - \Delta_L$  plane in the cases a)  $a > d_{c1}$  and b)  $a < d_{c1}$ .

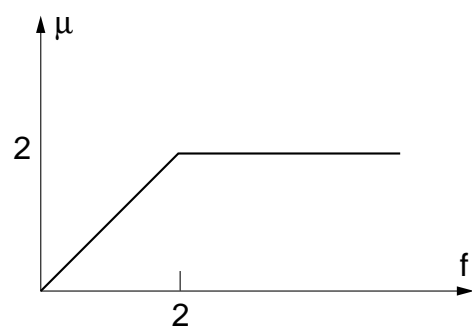
- 
- [1] D.S. Fisher in "Phase Transitions and Relaxations in Systems with Competing Energy Scales", NATO ASI Series, eds. T. Riste and D. Sherrington (Kluwer Academic Publishers, London, 1993)
  - [2] S. Alexander, J. Bernasconi, W.R. Schneider, and R. Orbach, Rev. Mod. Phys. **53**, 175 (1981)
  - [3] S. Havlin and D. ben-Avraham, Adv. Phys. **36**, 695 (1987)
  - [4] J.-P. Bouchaud and A. Georges, Phys. Rep. **195**, 127 (1990)
  - [5] W. Feller, *An Introduction to Probability Theory and its Applications* (Wiley, N.Y. 1971)
  - [6] T. Geisel, J. Nierwetberg, and A. Zacherl, Phys. Rev. Lett. **54**, 616 (1985)
  - [7] S. Grossman, F. Wegner, and K.H. Hoffmann, J. Phys. (Paris) Lett. **46**, L575 (1985)
  - [8] T. Bohr and A. Pikovsky, Phys. Rev. Lett. **70**, 2892 (1993)
  - [9] M. Sahimi, J. Phys. **A20**, L1293 (1987)
  - [10] M.F. Shlesinger and J. Klafter, Phys. Rev. Lett. **54**, 2551 (1985)
  - [11] H.C. Fogedby, T. Bohr, and H.J. Jensen, J. Stat. Phys. **66**, 583 (1992)
  - [12] H. Scher and E.W. Montroll, Phys. Rev. **B12**, 2455 (1974)
  - [13] M.F. Shlesinger, J. Stat. Phys. **10**, 421 (1974)
  - [14] S. Alexander and R. Orbach, J. Phys. (Paris) Lett. **43**, L625 (1982)
  - [15] A. Blumen, J. Klafter, B.S. White, and G. Zumofen, Phys. Rev. Lett. **53**, 1301 (1984)
  - [16] A. Blumen, J. Klafter, and G. Zumofen in *Optical Spectroscopy of Glasses*, edited by T. Zschokke (Reidel, Dordrecht, 1986), p. 199
  - [17] B.D. Hughes, M.F. Shlesinger, and E.W. Montroll, Proc. Natl. Acad. Sci. USA **78**, 3287 (1981)
  - [18] D.S. Fisher, Phys. Rev. **A30**, 960 (1984)
  - [19] B. Derrida and J.M. Luck, Phys. Rev. **B28**, 7183 (1983)
  - [20] J.M. Luck, Nucl. Phys. **B225**, 169 (1983)
  - [21] Ya. G. Sinai, in: Lecture Notes in Physics, Vol 153, eds. R. Schrader, R. Seiler, and D. Uhlenbrock (Springer, Berlin, 1981) and Ya. G. Sinai, Theor. Prob. Appl. **27**, 247 (1982)
  - [22] J. Klafter, A. Blumen, G. Zumofen, and M.F. Shlesinger, Physica A **168**, 637 (1990)
  - [23] A. Blumen, G. Zumofen, J. Klafter, Phys. Rev. **A40**, 3964 (1989)
  - [24] A. Ott, J.-P. Bouchaud, D. Langevin, and W. Urbach, Phys. Rev. Lett. **65**, 2201 (1990)
  - [25] H.C. Fogedby, Phys. Rev. Lett. **73**, 2517 (1994)
  - [26] J. Aronovitz and D.R. Nelson, Phys. Rev. **A30**, 1948 (1984)
  - [27] J.-P. Bouchaud, A. Comtet, A. Georges, and P. Le Doussal, J. Phys. (Paris) **48**, 1445 (1987), **49**, 369 (1988) (erratum)
  - [28] P. Lévy, *Théorie de l'Addition des Variables Aléatoires*, (Gauthier-Villars, Paris, 1937)
  - [29] B. B. Mandelbrot, *The Fractal Geometry of Nature* (W.H. Freeman, N.Y., 1982)
  - [30] M. F. Shlesinger, J. Klafter, and Y. M. Wong, J. Stat. Phys. **27**, 499 (1982)
  - [31] M. F. Shlesinger, J. Klafter, and B. J. West, Physica **140A**, 212 (1986)
  - [32] R. K. Pathria, *Statistical Mechanics*, (Pergamon, Oxford 1972)
  - [33] Power law noise has also been used in order to model disorder for moving interfaces, Y.-C. Zhang, J. Phys. (Paris) **51**, 2129 (1990)
  - [34] H. C. Fogedby, Phys. Rev. E **50** 1657 (1994)
  - [35] D. S. Fisher, D. Friedan, Z. Qiu, S. J. Shenker, and S. H. Shenker, Phys. Rev. **A31**, 3841 (1985)
  - [36] P. C. Martin, E. Siggia, and H. Rose, Phys. Rev. **A8**, 423 (1973)
  - [37] C. De Dominicis and L. Peliti, Phys. Rev. **B18**, 353 (1978)
  - [38] C. De Dominicis, Phys. Rev. **B18**, 4913 (1978)
  - [39] R. Bausch, H. K. Janssen, and H. Wagner, Z. Phys. **B24**, 113 (1976)
  - [40] L. Peliti and Y.-C. Zhang, J. Phys. **A18**, L709 (1985)
  - [41] S.-K. Ma and G. Mazenko, Phys. Rev. **B11**, 4077 (1975)
  - [42] S.-K. Ma, *Modern Theory of Critical Phenomena* (Benjamin, 1976)
  - [43] D. Forster, D. R. Nelson, and M. S. Stephen, Phys. Rev. Lett. **36**, 867 (1976), Phys. Rev. **A16**, 732 (1977)
  - [44] H. C. Fogedby and A. P. Young, J. Phys. **C11**, 527 (1978)
  - [45] H. C. Fogedby, *Theoretical Aspects of Mainly Low Dimensional Magnetic Systems*, Chapter V, Lecture Notes in Physics, Vol. 131 (1980)
  - [46] K. G. Wilson and J. Kogut, Phys. Rev. **12C**, 75 (1974)
  - [47] B. I. Halperin, P. C. Hohenberg, and S.-K. Ma, Phys. Rev. Lett. **29**, 1548 (1972), Phys. Rev. **B10**, 137 (1974)

- [48] E. Frey and U. C. Täuber, Phys. Rev. **E50**, 1024 (1994)
- [49] J. Honkonen and E. Karjalainen, J. Phys. **A21**, 4217 (1988)
- [50] J. Honkonen and E. Karjalainen, Phys. Lett. **129**, 333 (1988)
- [51] J. Honkonen and Yu. M. Pis'mak, J. Phys. **A22**, L899 (1989)
- [52] J. Honkonen, J. Phys. **A24**, L1235 (1991)
- [53] We note that introducing distinct fall-off exponents  $a_L \neq a_T$ , i.e.,  $\epsilon_L \neq \epsilon_T$ , the “degeneracy” is lifted and instead of a line of fixed points we only obtain the longitudinal fixed point
- [54] R. L. Stratonovich, *Topics in the theory of random noise*, Vol. 1 (Gordon and Breach, New York 1963)
- [55] E.W. Montroll and B. J. West in *Fluctuation Phenomena*, eds. E. W. Montroll and J. L. Lebowitz (North-Holland, New York 1987)

## Figure captions

- Fig. 1. Plot of the Lévy distribution for a microscopic step  $\eta$ . The tail of  $p(\eta)$  is characterized by the step index  $f$ . The distribution is cut off at a smallest step distance  $\eta_0$  corresponding to a microscopic length.
- Fig. 2. The scaling index  $\mu$  plotted as a function of the step index  $f$ .
- Fig. 3. Diagrammatic representation of the Fokker-Planck equation.
- Fig. 4. Diagrammatic representation of the Dyson equation defining the self energy  $\Sigma(\mathbf{k}, \omega)$  and the renormalized propagator  $G(\mathbf{k}, \omega)$ .
- Fig. 5. Diagrammatic representation of the renormalized Fokker-Planck equation.
- Fig. 6. Diagrammatic representation of the 4-point vertex function  $\Gamma(\mathbf{k}, \mathbf{p}, \mathbf{l}, \omega)$  and the contraction  $\int \Gamma(\mathbf{k}, \mathbf{k}, \mathbf{l}, \omega) G(\mathbf{k} - \mathbf{l}, \omega) d^d \ell / (2\pi)^d$ .
- Fig. 7. Diagrammatic representation of the first loop order correction to  $\Sigma(\mathbf{k}, \omega)$ .
- Fig. 8. Diagrammatic representation of the first loop order correction to  $\Lambda(\mathbf{k}, \mathbf{p}, \omega)$ .
- Fig. 9. Diagrammatic representation of the first loop order corrections to  $\Gamma(\mathbf{k}, \mathbf{p}, \mathbf{l}, \omega)$ .
- Fig. 10. Diagrammatic representation of the renormalized Fokker-Planck equation valid in the long wavelength region  $1 < k < e^{-\ell}$ . The slash indicates corrections evaluated on the shell  $e^{-\ell} < k < 1$ .
- Fig. 11. Plot of the critical dimension  $d_{c1}$  as a function of the scaling index  $\mu$ . For  $\mu = 2$  we have the Brownian case  $d_{c1} = 2$ ; for  $1 < \mu < 2$  the dimension  $d_{c1}$  depends linearly on  $\mu$ . The ballistic case  $\mu = 1$  is attained for  $d_{c1} = 0$ . The critical dimension  $d_{c1} = 2\mu - 2$  and the line  $d = \mu$  separate the regions I, II and II, III, respectively. In I the diffusion coefficient  $D_2$  vanishes and the disorder is *irrelevant*, in II  $D_2$  diverges and disorder is *irrelevant*, and in III  $D_2$  diverges and disorder becomes *relevant*.
- Fig. 12. Plot of the fixed point  $(\Delta^*, D_2^*)$  as a function of the scaling index  $\mu$  for  $1 + d/2 < \mu < 2$ .
- Fig. 13. Plot of the fall-off exponent as a function of the scaling index  $\mu$ . For  $\mu = 2$  we have the Brownian case. The lines  $a = \mu$  and  $a = 2\mu - 2$  separate the regions I, II and II, III, respectively. In I the diffusion coefficient  $D_2$  vanishes and the disorder is *irrelevant*, in II  $D_2$  diverges and disorder is *irrelevant*, and in III  $D_2$  diverges and disorder becomes *relevant*.
- Fig. 14. Plot of  $a$  versus  $d$ . The line  $a = d$  delimits the short range and long range regions. In region III for  $a > \mu$  and  $d > \mu$  the diffusion coefficient  $D_2$  vanishes and the disorder is *irrelevant*, in region II for  $\mu > d > 2\mu - 2$  and  $\mu > a > 2\mu - 2$   $D_2$  diverges and disorder is *irrelevant*, and in region III for  $0 < d < \mu$  and  $0 < a < \mu$   $D_2$  diverges and disorder becomes *relevant*.
- Fig. 15. Renormalization group flow in the  $\Delta - D_2$  plane about the Gaussian fixed point  $(\Delta^*, D_2^*) = (0, 0)$ . In case a)  $d > \mu$ , case b)  $d = \mu$ , and case c)  $d_{c1} < d < \mu$ . Fig. 16. **The anisotropic short range case:** Renormalization group flow in the  $\Delta_T - \Delta_L$  plane. Case a):  $d > d_{c1} = 2\mu - 2$  and the trajectories flow towards the stable Gaussian fixed point ( $G$ ) with constant slope. Case b):  $1 < d < d_{c1}$  and the trajectories flow towards the non-trivial isotropic fixed point ( $I$ ). Case c):  $d < 1$  and the trajectories flow towards the non-trivial longitudinal fixed point ( $A$ ).
- Fig. 17. **The anisotropic long range case:** Renormalization group flow in the  $\Delta_T - \Delta_L$  plane. Case a):  $a > d_{c1} = 2\mu - 2$  and the trajectories flow towards the stable Gaussian fixed point ( $G$ ) with constant slope. Case b):  $a < d_{c1} = 2\mu - 2$  and the trajectories flow towards the non-trivial line of fixed points ( $L$ ) with constant slope.





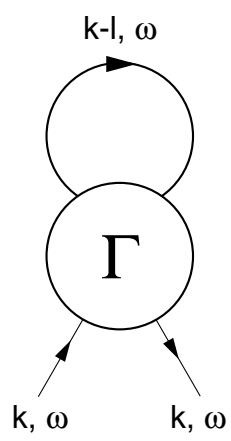
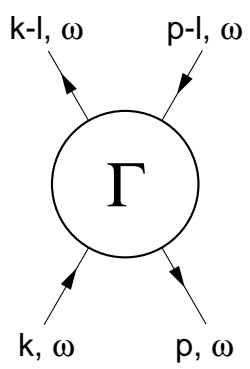
$$\begin{array}{c} \text{---} \text{ } k, \omega \text{ ---} \end{array} = \begin{array}{c} \text{---} k, \omega \text{ ---} \end{array} \blacktriangleright \chi + \begin{array}{c} \text{---} k, \omega \text{ ---} \end{array} \blacktriangleright \begin{array}{c} \text{E} \text{ } k-p \\ \text{ } \lambda_L \text{ } p, \omega \end{array} + \begin{array}{c} \text{---} k, \omega \text{ ---} \end{array} \blacktriangleright \begin{array}{c} \text{B} \text{ } k-p \\ \text{ } \lambda_T \text{ } p, \omega \end{array}$$

The diagram illustrates the decomposition of a photon propagator into its scalar and tensor components. On the left, a thick horizontal line represents the photon propagator with momentum  $k$  and frequency  $\omega$ . This is equal to the sum of three terms. The first term is a scalar propagator, represented by a thin horizontal line with an arrow pointing right, labeled  $\chi$ . The second term is a longitudinal tensor propagator, represented by a thin horizontal line with an arrow pointing right to a vertex. From this vertex, a wavy line labeled  $E$  with momentum  $k-p$  goes up and to the right, and a solid line labeled  $p, \omega$  goes down and to the right. The vertex is labeled  $\lambda_L$ . The third term is a transverse tensor propagator, represented by a thin horizontal line with an arrow pointing right to a vertex. From this vertex, a wavy line labeled  $B$  with momentum  $k-p$  goes up and to the right, and a solid line labeled  $p, \omega$  goes down and to the right. The vertex is labeled  $\lambda_T$ .

$$\overrightarrow{k, \omega} = \overrightarrow{k, \omega} + \overrightarrow{k, \omega} \circlearrowleft \Sigma \overrightarrow{k, \omega}$$

$$\begin{array}{c} \hline k, \omega \end{array} = \begin{array}{c} \hline k, \omega \end{array} \rightarrow x + \begin{array}{c} \hline k, \omega \end{array} \rightarrow \Lambda_L \begin{array}{l} \nearrow E \quad k-p \\ \searrow p, \omega \end{array} + \begin{array}{c} \hline k, \omega \end{array} \rightarrow \Lambda_T \begin{array}{l} \nearrow B \quad k-p \\ \searrow p, \omega \end{array}$$





$$\Sigma(k, \omega) =$$

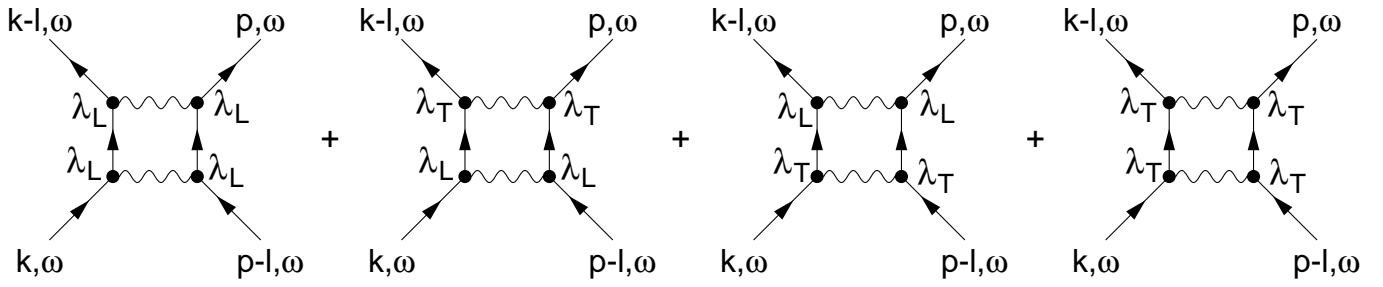
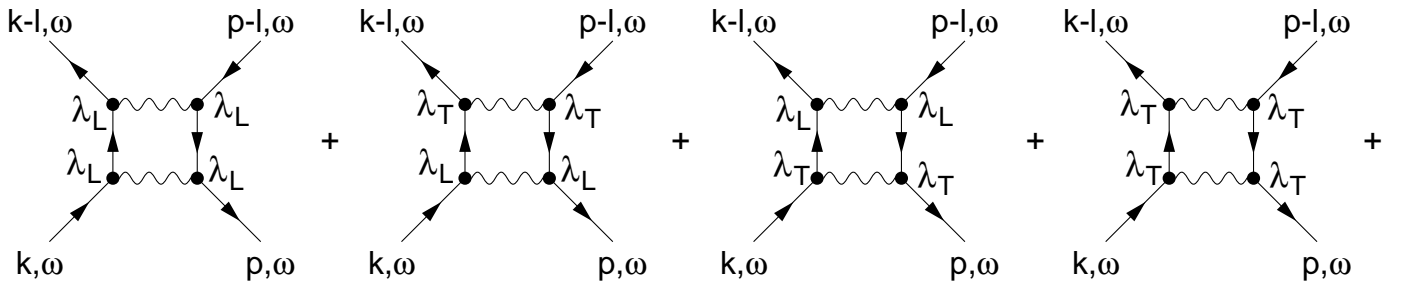
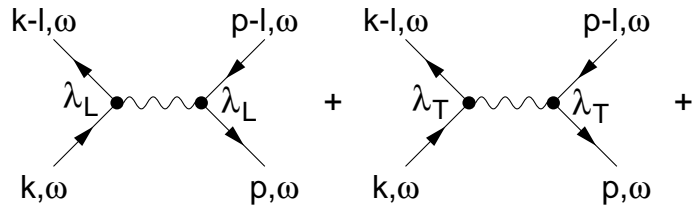
$$\begin{array}{c}
\Delta_L \\
\text{wavy line} \\
\frac{k}{2} - p \\
\text{solid line with arrow} \\
\lambda_L \quad \frac{k}{2} + p, \omega \quad \lambda_L
\end{array}
+
\begin{array}{c}
\Delta_T \\
\text{wavy line} \\
\frac{k}{2} - p \\
\text{solid line with arrow} \\
\lambda_T \quad \frac{k}{2} + p, \omega \quad \lambda_T
\end{array}$$

$$\begin{aligned}
\Lambda(k,p,\omega) = & \text{Diagram 1} + \text{Diagram 2} + \\
& \text{Diagram 3} + \text{Diagram 4} + \\
& \text{Diagram 5} + \text{Diagram 6}
\end{aligned}$$

The diagrams represent various Feynman-like diagrams for the polarization function  $\Lambda(k,p,\omega)$ . They are organized into three rows, each containing two diagrams separated by a plus sign.

- Row 1:**
  - Diagram 1: An incoming horizontal line with momentum  $k, \omega$  and wavelength  $\lambda_L$  enters a vertex. From this vertex, a wavy line labeled  $E$  goes up and to the right, and another line with momentum  $p, \omega$  and wavelength  $\lambda_L$  goes down and to the right.
  - Diagram 2: Similar to Diagram 1, but the wavy line is labeled  $B$  and the wavelength of the outgoing line is  $\lambda_T$ .
- Row 2:**
  - Diagram 3: An incoming horizontal line with momentum  $k, \omega$  and wavelength  $\lambda_L$  enters a vertex. A wavy line labeled  $E$  goes up and to the right. A second vertex is reached by a wavy line from the first vertex, with wavelength  $\lambda_L$  and a label  $I$  below it. From the second vertex, a line with momentum  $p, \omega$  and wavelength  $\lambda_L$  goes down and to the right.
  - Diagram 4: Similar to Diagram 3, but the wavy line is labeled  $E$  and the wavelength of the outgoing line is  $\lambda_T$ .
- Row 3:**
  - Diagram 5: An incoming horizontal line with momentum  $k, \omega$  and wavelength  $\lambda_L$  enters a vertex. A wavy line labeled  $B$  goes up and to the right. A second vertex is reached by a wavy line from the first vertex, with wavelength  $\lambda_T$  and a label  $I$  below it. From the second vertex, a line with momentum  $p, \omega$  and wavelength  $\lambda_L$  goes down and to the right.
  - Diagram 6: Similar to Diagram 5, but the wavy line is labeled  $B$  and the wavelength of the outgoing line is  $\lambda_T$ .

$$\Gamma(k,p,l,\omega)=$$



$$\begin{aligned}
 & \text{---} = \text{---} \rightarrow \times + \text{---} \rightarrow \text{---} + \text{---} \rightarrow \text{---} + \\
 & \text{---} \rightarrow \text{---} + \text{---} \rightarrow \text{---} + \\
 & \text{---} \rightarrow \text{---} + \text{---} \rightarrow \text{---}
 \end{aligned}$$

The image displays a series of Feynman diagrams representing a perturbative expansion. The first line shows a thick horizontal line (representing a fermion) equal to a sum of four terms: a thin line with an arrow pointing to a cross, a thin line with an arrow pointing to a thick line, a thin line with an arrow pointing to a thick line with a wavy line loop, and a thin line with an arrow pointing to a thick line with a wavy line loop and a vertical line. The second line shows a thin line with an arrow pointing to a thick line with a wavy line loop, followed by a plus sign and a thin line with an arrow pointing to a thick line with a wavy line loop and a vertical line, followed by a plus sign. The third line shows a thin line with an arrow pointing to a thick line with a wavy line loop, followed by a plus sign and a thin line with an arrow pointing to a thick line with a wavy line loop and a vertical line.

